Photofission studies with the ELIGANT-TN instrument
Technique Development
GANT-PhotoFiss

Dan Filipescu [1] Ioana Gheorghe [1] Anabella Tudora [2]

[1]Horia Hulubei National Institute for R&D in Physics and Nuclear Engineering (IFIN-HH)

[2]Faculty of Physics, University of Bucharest

07 November 2023

Overview

1. General introduction
2. Goal of the project
   - Photofission with ELIGANT-TN – Technique Development
   - Method validation on NewSUBARU ^{238}U and ^{232}Th photofission data
3. Team members and project costs
4. Work done during 2020 – 2023
   - 2020 – Preliminary stage of ^{238}U and ^{232}Th photofission data analysis and modeling of prompt neutron emission
     - I.1. Development of algorithm for format conversion of raw experimental data
     - I.2. Modeling of prompt fission neutron emission multiplicity distribution
   - 2021 – Preliminary stage of ^{238}U and ^{232}Th photofission data analysis and modeling of prompt neutron emission
     - II.1. Characterization of incident gamma ray beam
     - II.2. Modeling of prompt fission neutron emission energy spectra
   - 2022 – Photofission data analysis - developing the method and applying to experimental data
     - III.1. Dedicated neutron detection efficiency determination
     - III.2. Neutron multiplicity sorting method dedicated for photofission - development and application to experimental data
     - III.3. Energy unfolding of excitation functions and average energies of neutron spectra for ^{238}U and ^{232}Th
   - 2023 – Statistical model evaluations of photon induced reactions on ^{238}U and ^{232}Th
     - IV.(1) Additional work: Investigate effects of fission induced by PFN emitted in photofission
     - IV.(2) Additional work: first- and second-chance fission separation
     - IV. Statistical model calculations
5. Future plans
6. Summary

General introduction – Photofission at the GDR energy region

- The photoabsorption cross section is known to be dominated by the electric dipole (E1) mode in the γ-ray energy region of $\sim S_n$ to $\sim$20 MeV characterizing the well-known Giant Dipole Resonance (GDR).
- Starting with medium mass nuclei, the height of the Coulomb barrier restricts charged particle emission decays of the GDR.
- For actinide nuclei, the photoabsorption cross section can thus be well approximated with the sum cross section of the photofission and photoneutron (γ, n), $(\gamma, 2n)$, ... reactions.
- A simultaneous reproduction of the competing photoneutron (γ, n), $(\gamma, 2n)$, ... as well as the first- (γ, f), second- (γ, nf), ... chances photofission cross sections can be a valuable tool in validating the consistency and reliability of the fission barrier parameters and the states at super- and hyper-deformations.

- Starting with the 1960's, photoneutron cross section measurements in the GDR region had been routinely performed at the Saclay and Livermore positron in flight annihilation facilities by multiplicity sorting of coincidence neutron detection events from (γ, xn) reactions with $x = 1, 2, 3$. Many of the existing data on photoabsorption cross sections in the GDR region have been produced at these two facilities.
- Systematic discrepancies still unresolved are however present between the Saclay and Livermore data sets
- The main experimental challenge in the Saclay and Livermore neutron multiplicity sorting investigations of photonuclear reactions in the GDR region was to discriminate the photofission emission from the photoneutron one for incident photon energies above the neutron separation energy.

Section 2

Goal of the project

Photofission with ELIGANT-TN – Technique Development

- The mission of the GANT-PhotoFiss project is to develop a new technique for simultaneous photofission and photoneutron cross section measurements with the ELI-NP Gamma Above Neutron Threshold Thermal Neutrons (ELIGANT-TN) detection setup, along with the associated LCS γ-ray beam diagnostics procedures.
  - Currently, only Fission Fragment detection experiments are planned in the photofission programme at ELI-NP, providing information on photofission cross-sections and mass, charge, angular, and kinetic energy distributions. Although the foreseen scientific output is highly interesting for describing the process of nuclear fission, the current ELI-NP photofission programme includes no investigation on the Prompt Fission Neutron (PFN) emission critical nuclear data required by nuclear applications.
- Project GANT-PhotoFiss will develop a method for measuring photofission cross sections and PFN multiplicity distribution and PFN average energy spectra by using the Flat Efficiency Detector ELIGANT-TN. The ELIGANT-TN instrument was initially developed by the ELIGANT group for photoneutron measurements and it is currently fully functional and commissioned. We will produce a ready to use algorithm for combined photofission and photoneutron Day 1 experiments at the ELI-NP Gamma Beam System. The algorithm will be applied for validation on ^{238}U and ^{232}Th photofission data sets measured in the Giant Dipole Resonance region at the NewSUBARU Laser Compton Scattering γ-ray beam facility.

Method validation on NewSUBARU ^{238}U and ^{232}Th photofission data

Laser Compton scattering (LCS) γ-ray beams at NewSUBARU

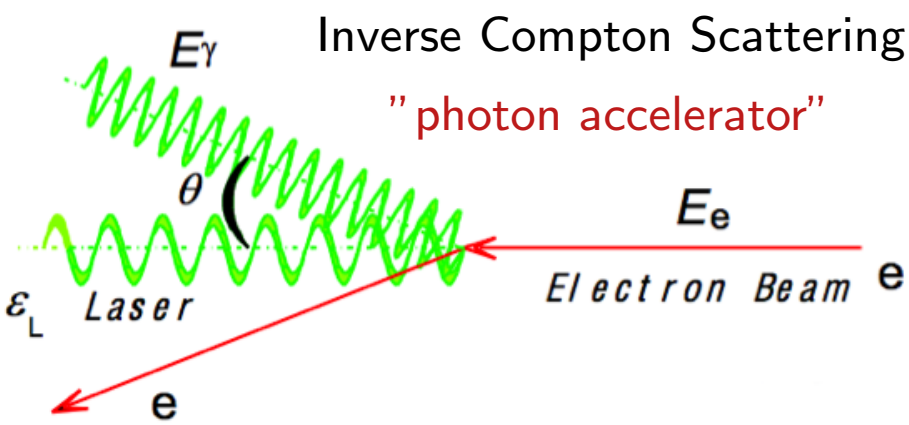

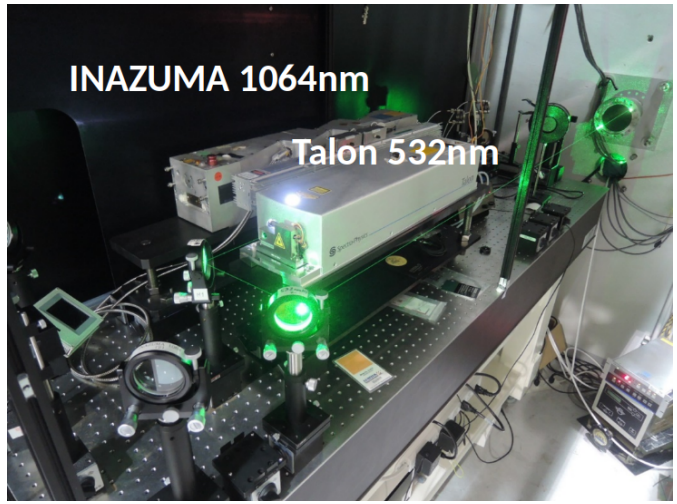

5.86 MeV$\leq$E$_\gamma\leq$20.12 MeV
using:

- 1064nm Nd:YVO_4 Navigator II laser
  Q-switch @ 1 kHz (1 ms. interval) & 40 ns. wide
- 589.89 to 1071.78 MeV (10^{-5} accuracy) electrons @ 500 MHz (2 ns. interval) & 60 ps. width
- double 10 cm thick Pb collimators of 3 and 2 mm diameter apertures

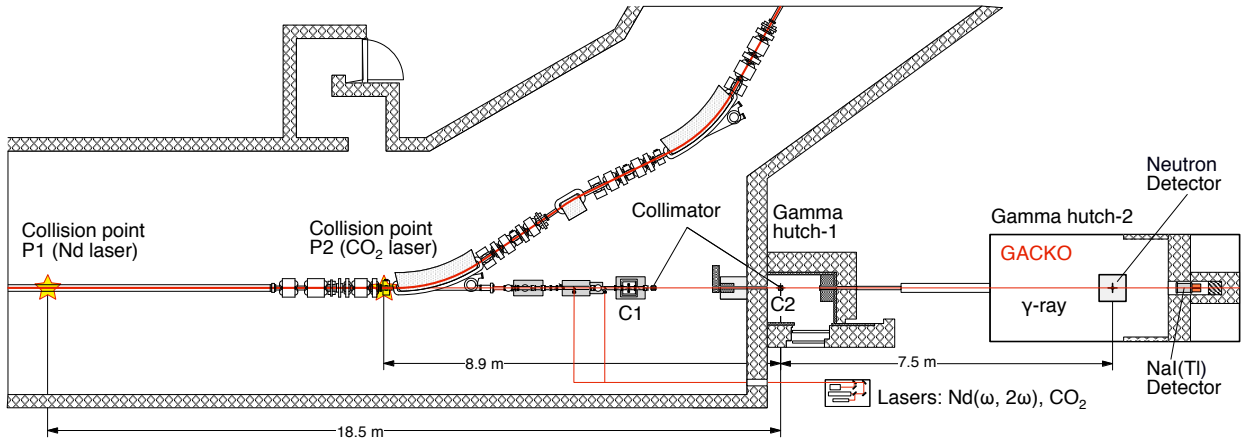

Section 3

Team members and project costs

Section 3. Team members and project costs

First Name, Last Name	Academic Degree	Realized FTE 2020	Realized FTE 2021	Realized FTE 2022	Realized FTE 2023
Dan FILIPESCU	Dr., CSII	0.15	0.16	0.27	0.15
Ioana GHEORGHE	Dr., CS	0.15	0.16	0.05	0
Cristina CLISU	PhD student	0	0.64	0.25	0.09
Sorin UJENIUC	PhD student	0	0	0	0
Anabella TUDORA	Prof. Univ. Dr.	0.03	0.09	0.10	0.03

	TOTAL	2020	2021	2022	2023
Allocated budget:	750.000,00 lei	100.000,00	275.000,00	300.000,00	75.000,00
Realized budget:	750.000,00 lei	100.000,00	275.000,00	300.000,00	75.000,00

Section 4

Work done during 2020 – 2023

Subsection 1

2020 – Preliminary stage of ^{238}U and ^{232}Th photofission data analysis and modeling of prompt neutron emission

I.1. Development of algorithm for raw experimental data format conversion

- λ=1064 nm laser operated in Q-switch mode triggered by:
  - 1 kHz logic signal
  - *slow* 10 Hz logic signal for background subtraction (80 ms beam-on / 20 ms beam-off)
- reaction neutrons recorded by moderated neutron detection array composed of 3 concentric rings of 31 ^{3}He counters. Each ring was connected to an OR logical electronic system.
- LCS γ-ray flux monitored with 8in$\times$12in NaI(Tl) detector which produced a pile-up signal for each multiple photon pulse recorded.
- LCS γ-ray beam spectra monitored with 3.5in$\times$4in $LaBr_3$ detector.
- DAQ recorded: time of detection relative to the beginning of the irradiation – on 64 bits (40 ns time unit) and the amplitude of the signal. DAQ Input configuration:
  - Ch1. 1 kHz clock signal (TTL)
  - Ch2. 10 Hz clock signal (TTL)
  - Ch3. General neutron OR signal (TTL)
  - Ch4. Inner ring – Pair 1 (TTL)
  - Ch5. Inner ring – Pair 2 (TTL)
  - Ch6. Middle ring (TTL)
  - Ch7. Outer ring (TTL)
  - Ch8. NaI amplitude signal
- We developed a code to organize the recorded data in an event mode format where the time range of an event is 1 ms – the interval of the LCS γ-ray pulse. The 1 kHz laser triggering signal was used to mark the beginning of the event and the slow 10 Hz signal to discriminate between beam ON – beam OFF events.

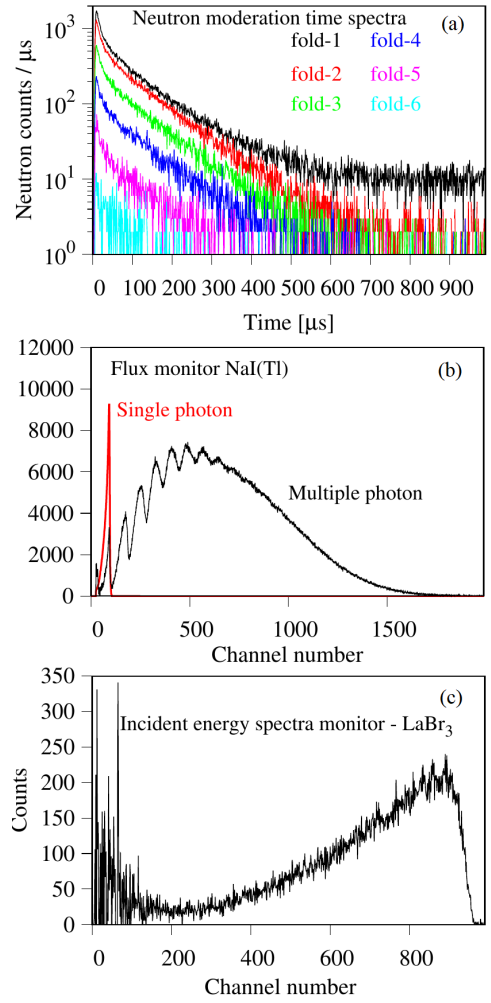

I.2. Modeling of prompt fission neutron emission multiplicity distribution

Terrel formalism: Gaussian distribution for P(ν).
Fitted the P(ν) for nine fission cases studied experimentally: ^{235}U(n$_{th}$,f), ^{239}Pu(n$_{th}$, f), ^{252}Cf(SF), ^{240}Pu(SF), ^{236}Pu(SF), ^{244}Cm(SF), ^{242}Pu(SF), ^{238}Pu(SF), ^{248}Cm(SF) and the corresponding PbP calculations. Linear behavior has been obtained for the $< \nu >$ and σ parameters as a function of <TXE>.

Characterized the <TXE> for the fissioning nuclei ^{238}U and ^{232}Th at the 5 MeV < E* < 21 MeV excitation energies:

$$< TXE >=< Q > +E* - < TKE >$$

where <Q> is the average energy release in fission (Q-value) and <TKE> is the average total kinetic energy of fission fragments. <TXE> obtained by the following steps:

1. Point by point (PbP) calculation of the energy release distribution Q(A).
2. Description of the TKE(A) distribution using experimental ^{238}U(n,f) and ^{232}Th(n,f) data.
3. GEF model code (General description of the fission process) calculation of the Y(A) distributions for ^{237}U(n,f) and ^{231}Th(n,f) performed at the neutron energy values which lead to the same E* as those of ^{238}U(n,f) and ^{232}Th(n,f) for which experimental TKE(A) data exist.

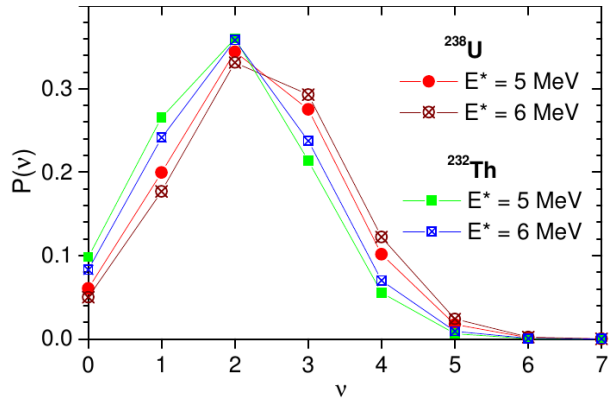

Examples of P(ν) for ^{238}U fissioning at E* = 5 MeV and E* = 6 MeV and of ^{232}Th fissioning at E* = 5 MeV and E* = 6 MeV based on the systematics of $<\nu>$(TXE) and σ (TXE) entering the Terrell expression of the cumulative P(ν) and on the systematic of <TXE>(E*).

The total average values of <Q> and <TKE> were obtained by averaging the distributions Q(A) (step 1) and TKE(A) (step 2) over the Y(A) distributions (step 3).
<TXE> was thus expressed as a function of excitation energy E* with a linearly increasing behavior.

Section 4

Work done during 2020 – 2023

Subsection 2

2021 – Preliminary stage of ^{238}U and ^{232}Th photofission data analysis and modeling of prompt neutron emission

II.1. Characterization of incident gamma ray beam - Flux

Poisson-fitting method:

$$N_{\gamma}^{\mathrm{det}} = \frac{\langle ch_{\mathrm{multiple-photon}} \rangle}{\langle ch_{\mathrm{single-photon}} \rangle} \cdot \Big(Area \Big)_{\mathrm{multiple-photon}}$$

During each irradiation, multiple photons emitted in ∼40ns long pulses are recorded simultaneously by the 8" × 12" NaI(Tl) detector, generating so called pile-up or multiple-photon spectra.

Time variation of incident γ-ray beam due to:

- electron beam current decay
- laser power fluctuations

This has to be characterized in order to assess multiple firing of photonuclear reactions induced by γ-ray pulses in the target. Thus, long irradiation run data was split into shorter time intervals during which the photon multiplicity can be well described by a Poisson distribution of mean:

$$m(k) = N^{det}(k)/N_{\gamma p}(k),$$

where k = time window index, N^{det}(k) = number of detected photons and $N_{\gamma p}$(k) = number of photon pulses.

Figure: reproduction of experimental incident photon multiplicity distributions with simulated Poisson distributions. The 5.86 MeV run is divided into 12 time windows. The average number of photons per pulse for each time window varies from 2.8 to 4.6 (displayed in the legend).

▸ H. Utsunomiya NIM A **896** (2018) 103

gives recent developments on treating:

- time variable incident flux
- quenching corrections for multiple photon spectra

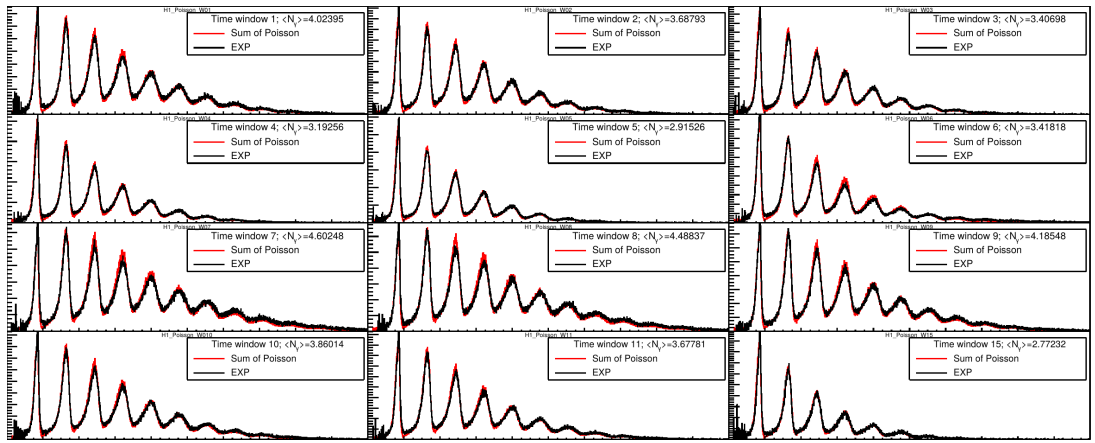

II.1. Characterization of incident gamma ray beam - Energy spectra

Quasi-monochromatic spectra (1∼3% FWHM energy resolution) obtained by selecting through collimation the high-energy, back-scattered Compton spectrum component.

- 3.5" ×4.0" $LaBr_3$:Ce monitor detector. The incident spectral distributions are obtained by reproducing the experimental detector response by simulations.
- **GEANT4 Monte Carlo simulation code for LCS γ-ray beam production&transport** developed for characterization of the scattered γ-ray photon beams, considering continuous, unsynchronized laser and electron beams.
- **Electron beam**: Gaussian emittance profile; Twiss parameters formalism is used to describe the electron beam phase space distribution along the interaction region.
- **Laser beam**: modeled as a Gaussian beam.
- Laser beam is aligned with electron beam → laser-electron overlap (gamma beam luminosity) presents high peak around laser focus.

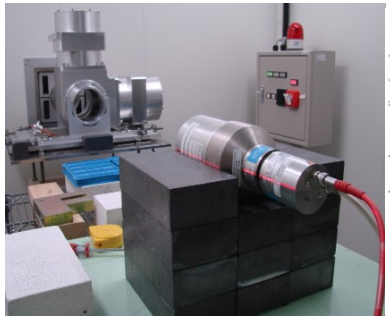

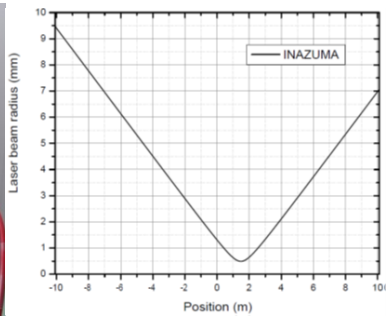

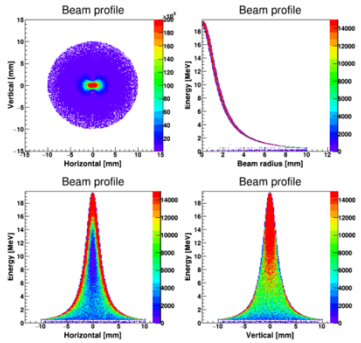

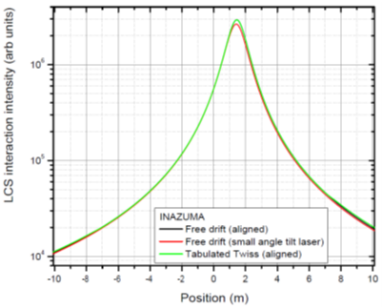

GANT-PhotoFiss publications on modeling LCS γ-ray sources for beam diagnostics:

- D. Filipescu et al., Spectral distribution and flux of LCS γ-ray beams, NIM A **1047**, 167885 (2023), arXiv:2211.14650
- D. Filipescu, Monte Carlo simulation of polarization effects in LCS on relativistic electrons, JINST **17** P11006 (2022), arXiv:2210.14669
- Takashi Ari-Izumi et al., Spatial distribution of collimated LCS γ-ray beams, JINST **18** T06005 (2023), arXiv:2304.08935

II.1. Characterization of incident gamma ray beam - Energy spectra

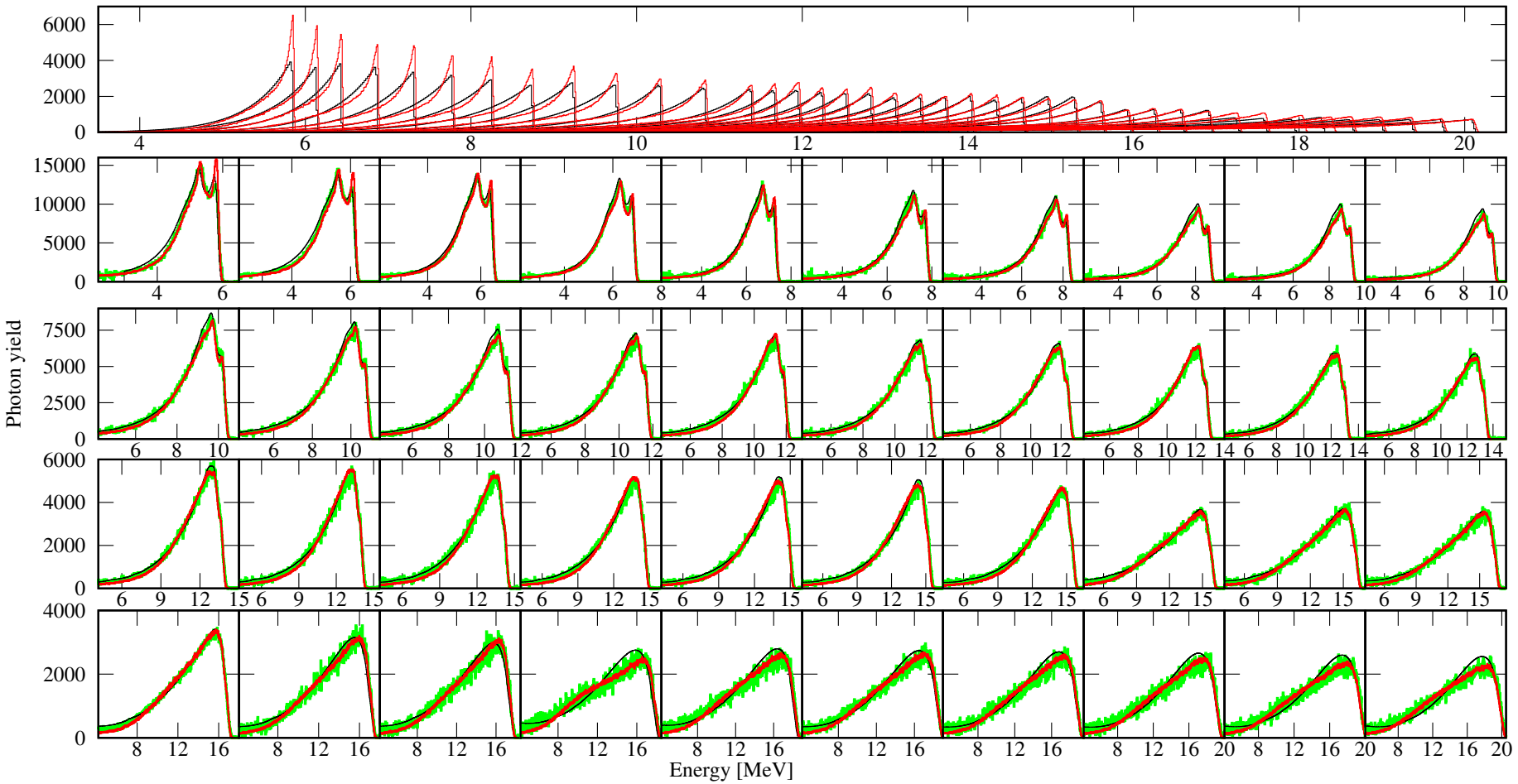

- Green: experimental $LaBr_3(Ce)$ spectra.
- Black: numerical unfolding.
- Red: LCS γ-ray beam simulation implemented in the Geant4 package.

II.1. Characterization of incident gamma ray beam - Energy spectra

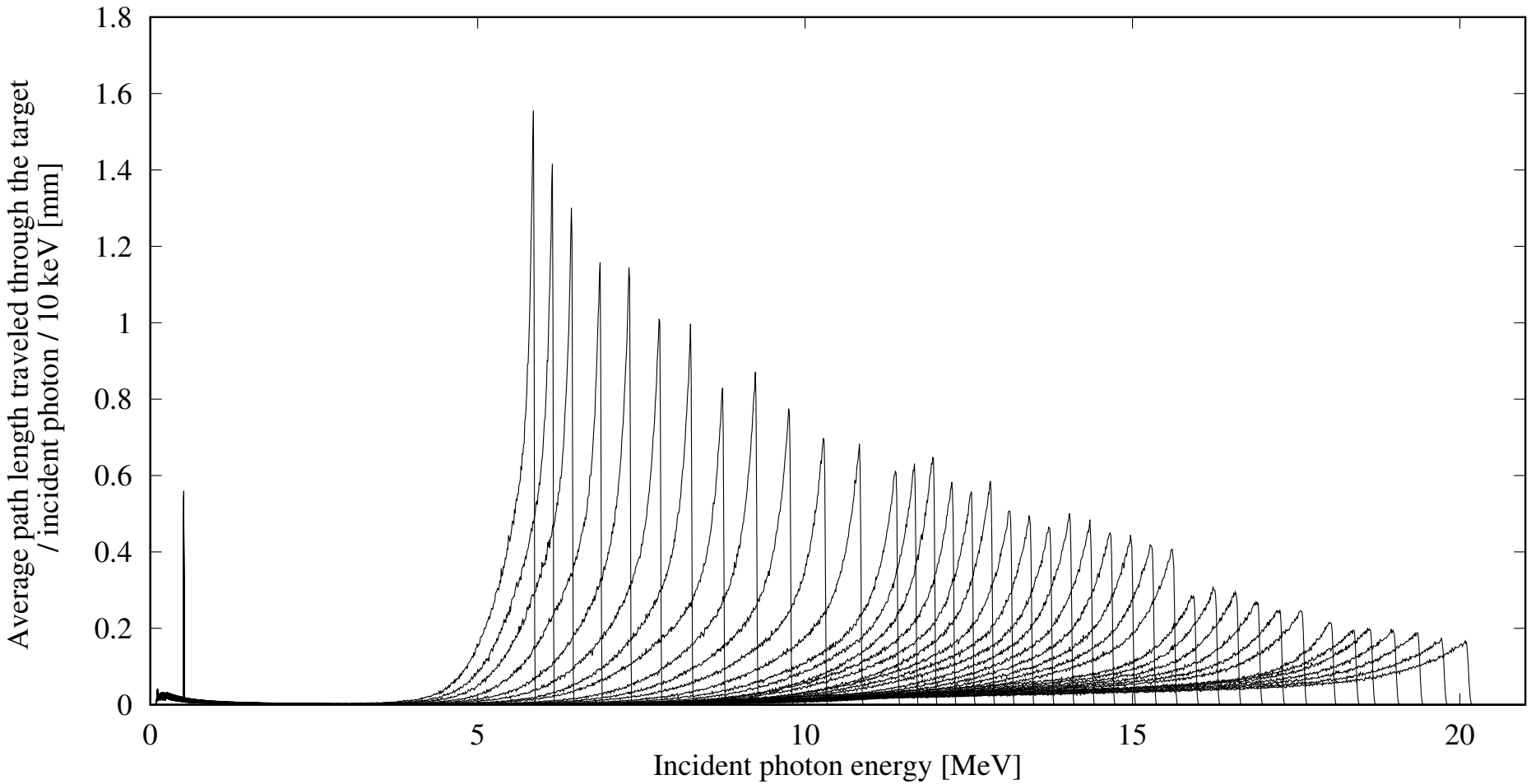

In order to model the secondary photon production in the target and asses their contribution to the measured reaction yield, we use the $L(E_\gamma, E_m)$ distribution defined as the average path length per unit energy traveled through the target by a E_γ photon in a LCS γ-ray beam of E_m maximum energy.

II.2. Modeling of prompt fission neutron emission energy spectra

In lack of experimental information on fission fragments and the prompt emission quantities of the fissioning nuclei ^{238}U and ^{232}Th, we predicted the prompt neutron spectra of γ + ^{238}U and ^{232}Th at incident energies E_γ ranging from 4 to 22 MeV by the most probable fragmentation approach (known as the Los Alamos (LA) model) with input parameters provided by systematics. We employed the LA version of Madland and Kahler ▸ NPhysA-957-289(2017) which consider different residual temperature distributions of the light and heavy fragment and the recent systematic of its input parameters ▸ A.Tudora EPJA-56-225(2020).
At $E_\gamma \leq 12$ MeV, the spectra of prompt neutrons emitted only from the fission fragments of the main nucleus undergoing fission were considered. At higher E_γ, multiple fission chances occur, so that the contributions of both, the prompt neutrons emitted from the fission fragments of each fissioning nucleus formed at the respective E_γ and of the so-called pre-fission neutrons were taken into account. At E_γ up to 22 MeV only the fissioning nuclei of the main chain are involved (i.e. $^{238-236}$U, $^{232-230}$Th), their average excitation energies (at which the prompt emission calculations are performed) given by iterative equations
▸ A.Tudora NSE-192-52(2018)

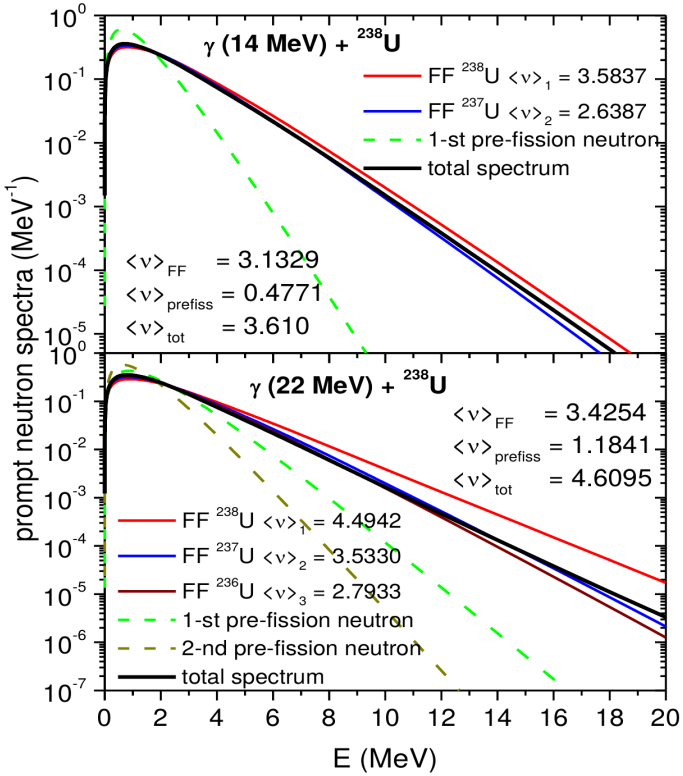

Prompt neutron spectra of the of γ + ^{238}U at E_γ = 14 MeV (upper part) and 22 MeV (lower part). Individual spectra of prompt neutrons emitted from the fission fragments of each fission chance are plotted with thin solid lines and the spectra of each pre-fission neutron with dashed lines. The total spectrum is plotted with a thick black line. The average prompt neutron multiplicity of each fission chance and the total average prompt neutron numbers $< \nu >_{FF}$, $< \nu >_{prefis}$ and $< \nu >_{tot}$ (as their sum) are given in the figure legends, too.

Section 4

Work done during 2020 – 2023

Subsection 3

2022 – Photofission data analysis - developing the method and applying to experimental data

III.1. Dedicated neutron detection efficiency determination

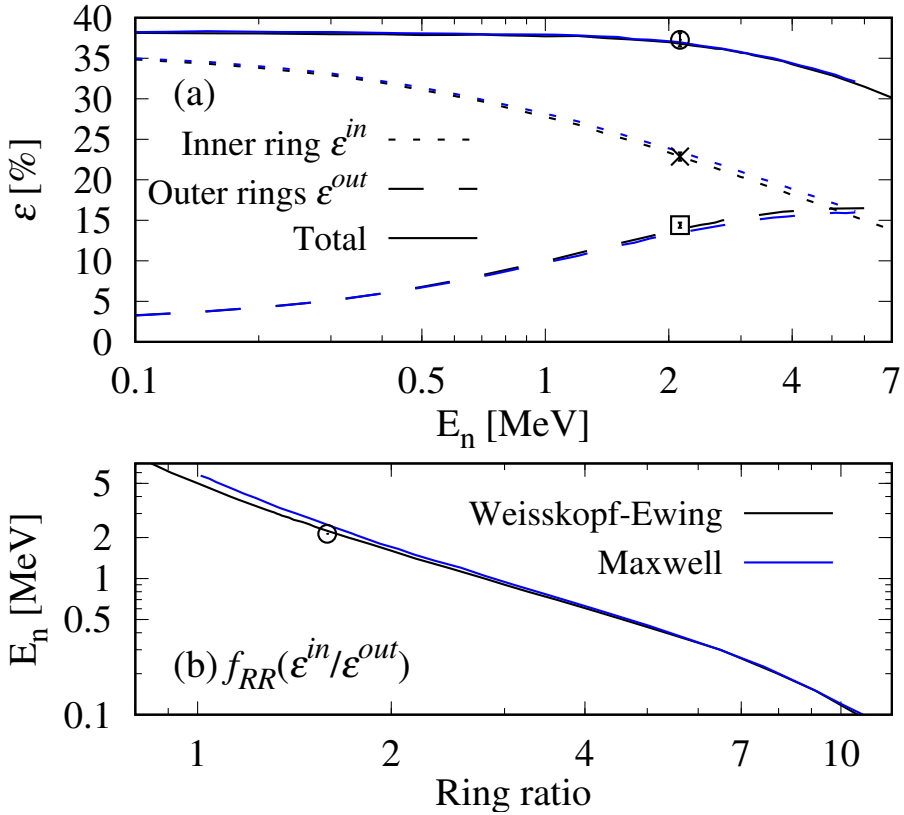

(a) Total detection efficiency (solid) and efficiencies of the inner (dotted) and outer (dashed) rings of the FED obtained by MCNP simulations for neutron evaporation spectra (black), Maxwell spectra (blue) & experimental ^{252}Cf calibration. (b) Ring ratio curves defined as inner ring / outer rings.

▸ H. Utsunomiya, I. Gheorghe, et. al, NIM A 871, 135-141 (2017)

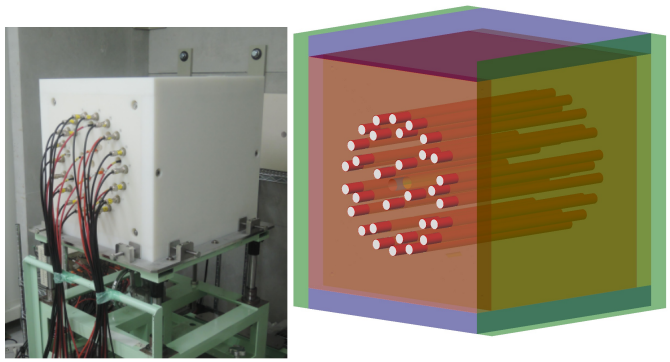

Flat detector response: average $\langle\varepsilon\rangle_{FED} = 36.5\pm1.6\%$; variation 38 $\sim$ 33% in the 10 keV to 5 MeV energy range typical for evaporation photoneutrons and PFN. Measured cross sections are insensitive to the neutron emission spectra.

neutron fold	efficiency
1 neutron	ε=$\sim$38%
2 neutrons	ε^2=$\sim$14%
3 neutrons	ε^3=$\sim$5.5%
4 neutrons	ε^4=$\sim$2%
i neutrons	ε^i=small

III.2. Neutron multiplicity sorting method dedicated for photofission - development and application to experimental data

- Neutron multiplicity counting
- Updated neutron-multiplicity sorting method
- Neutron coincidence events - *i*-fold cross sections
- Photoneutron and photofission contributions to neutron coincidence events
- PFN multiplicities predicted by the theory of evaporation in sequential neutron emission from excited nuclei – J.Terrell, Phys.Rev.**108**, 783 (1957)
- Energy dependent multiple-firing (MF) sorting method

III.2. Neutron multiplicity counting

Figure: Typical arrival-time distributions of neutrons recorded by the FED in neutron-multiplicity sorting experiments. Experimental neutron counts recorded during beam-on (black) and beam-off (red) and the best fit to the beam-on distribution (cyan).

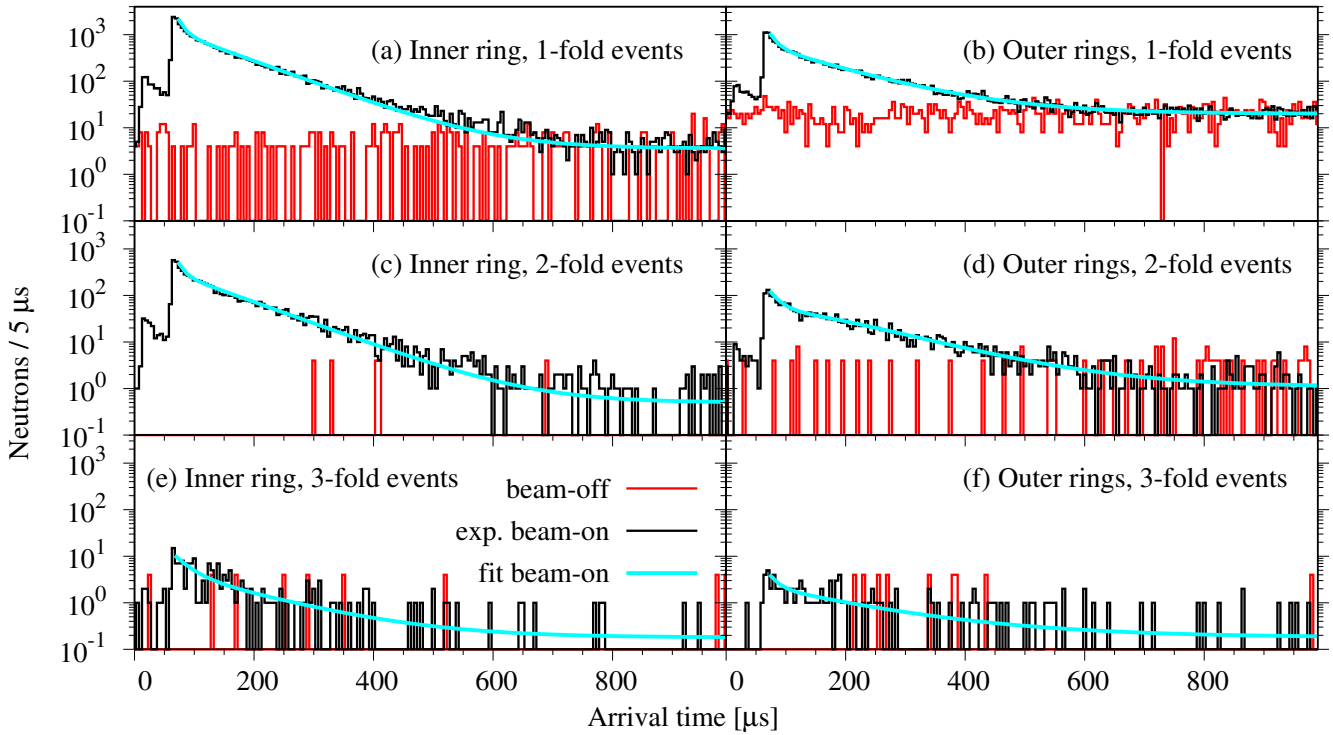

Background subtraction: laser had also a slow 10 Hz time structure of

80 ms beam-ON / **20 ms beam-OFF**.

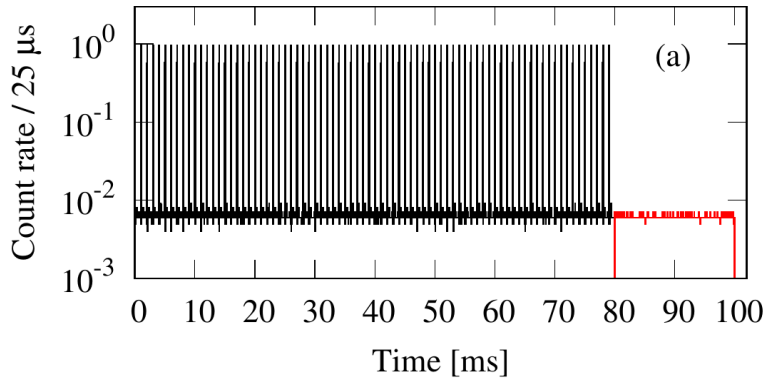

III.2. Updated neutron-multiplicity sorting method

Experimental observables:

- ***i*-fold cross section** N_i = the number of i-fold photoneutron events recorded per incident photon and target nucleus:

$$N_i = \frac{\sum_t (n_i^{in}[t] + n_i^{out}[t])/i}{N_\gamma n_T \xi}$$

  where $n_i^{in}[t]$ and $n_i^{out}[t]$ are the background subtracted arrival time histograms for neutrons detected in i-fold events by the inner ring and by the summed two outer rings, respectively. n_T is the concentration of target nuclei, N_γ is the incident photon number for the total irradiation time and $\xi = [1 - \exp(-\mu L)]/\mu$ is a thick target correction factor given by the target thickness L and attenuation coefficient μ.

- ***i*-fold average neutron energies** E_i determined by the RR method as $E_i = f_{RR}(\sum_t n_i^{in}[t] / \sum_t n_i^{out}[t])$.

III.2. Neutron coincidence events - *i*-fold cross sections

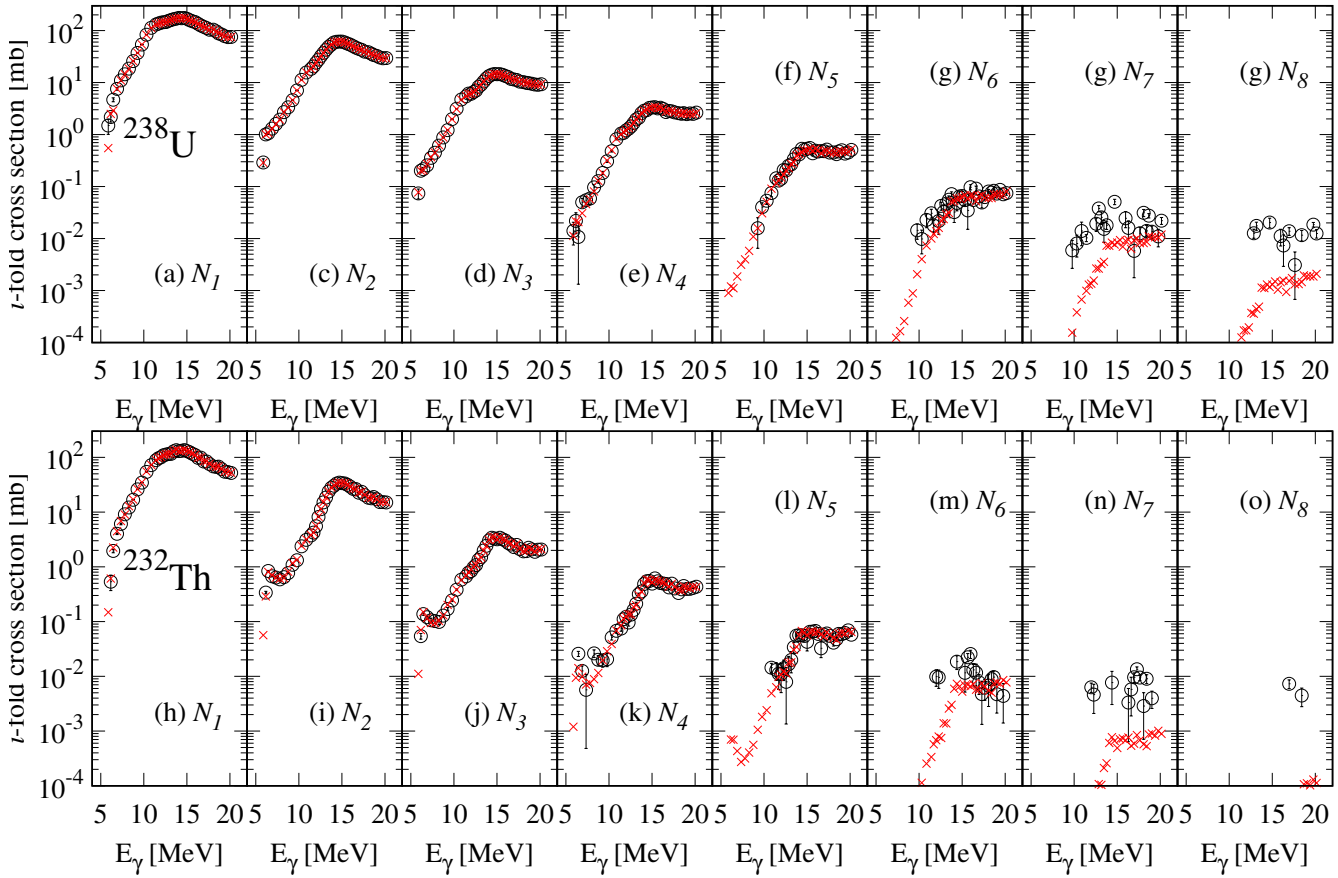

Experimental (N_i, empty black dots) and calculated (N_i^{MF}, red crosses) *i*-fold cross sections, defined as the number of *i*-fold neutron events recorded per incident photon and target nucleus, for the photoneutron and photofission reactions on ^{238}U (a – g) and ^{232}Th (h – o).

III.2. Photoneutron & photofission contributions to neutron coincidences

Competing reactions for actinide target irradiation with a γ-ray beam of energy $S_{2n} < E < S_{3n}$:

- photoneutron $(\gamma,\ n)$, $(\gamma,\ 2n)$
- photofission $(\gamma,\ f\ in)$ with emission of i neutrons, $0 \leq i \leq \nu_{max} \simeq 9$

For non-unity detection efficiency ε and *single-firing* conditions (no more than one nuclear reaction induced by the same photon pulse), the recorded N_1, N_2, ... N_k coincidences of 1, 2, respectively k neutrons are expressed as:

k-fold coincidence events	contributing reactions
$N_1 \sim \sigma_{(\gamma,\,n)} \cdot \varepsilon + \sigma_{(\gamma,\,2n)} \cdot 2\varepsilon(1-\varepsilon) + \sigma_{(\gamma,\,f)} \sum_{i=1}^{\nu_{max}} P_i \cdot {}_iC_1 \varepsilon (1-\varepsilon)^{i-1}$	$(\gamma,\ n)$, $(\gamma,\ 2n)$, $(\gamma,\ f\ in)$ with i ≥ 1
$N_2 \sim \sigma_{(\gamma,\,2n)} \cdot \varepsilon^2 + \sigma_{(\gamma,\,f)} \sum_{i=2}^{\nu_{max}} P_i \cdot {}_iC_2 \varepsilon^2 (1-\varepsilon)^{i-2}$	$(\gamma,\ 2n)$, $(\gamma,\ f\ in)$ with i ≥ 2
$N_k \sim \sigma_{(\gamma,\,f)} \sum_{i=k}^{\nu_{max}} P_i \cdot {}_iC_k \varepsilon^k (1-\varepsilon)^{i-k}$	$(\gamma,\ f\ in)$ with i ≥ 3

with P_i the probability to emit i neutrons in a fission event.

CHALLENGES:

- Because of non-unity detection efficiency, maximum order of detected neutrons is lower than $\nu_{max} \implies$ incomplete system of k equations with ν_{max} variables!
- Discrimination of the photoneutron $(\gamma,\ n)$, $(\gamma,\ 2n)$ and photofission contributions to the 1- and 2-fold neutron coincidence events.

SOLUTION: Description for the PFN multiplicity emission!

III.2. PFN multiplicities predicted by the theory of evaporation in sequential neutron emission from excited nuclei – J.Terrell, Phys.Rev.**108**, 783 (1957)

Two simplifying assumptions are made in the work of Terrell:

1. the emission of each neutron from any fission fragment is made by exhausting a ΔE energy value which is very close to the average value $E_0 \approx \overline{\Delta E}$;

2. the total excitation energy of the prompt fission fragments has a Gaussian distribution with a σE_0 deviation from an average excitation energy $\overline{E}$. Under these reasonable assumptions, Terrell demonstrates that the multiplicity distribution of the prompt fission neutrons can be approximated with a Gaussian depending only on two parameters: $\overline{\nu}$, the average number of prompt neutrons emitted per fission act and σ, the rms width of the total excitation energy distribution expressed in units of the E_0 average excitation energy cost per emitted neutron.

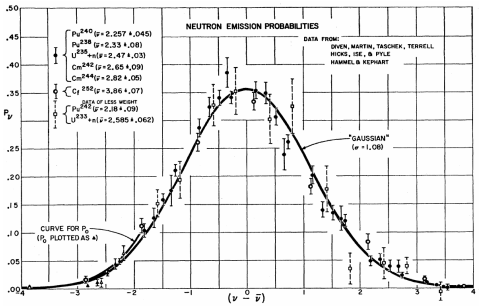

Fig. 4. Experimental noncumulative neutron emission probabilities. The continuous curves are for a "Gaussian" distribution. Experimental data are from references 14–16; standard deviations are shown.

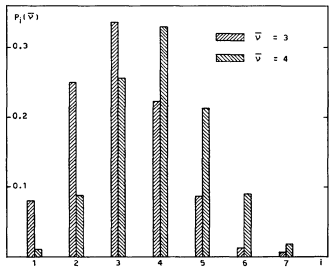

Fig. 2. Typical probability distribution $P_i[\bar{\nu}(E)]$ for a fissile nucleus to emit exactly i neutrons when breaking up at an excitation energy E with the emission of an average number of neutrons $\bar{\nu}$. The histograms correspond to $\bar{\nu}(E) = 3$ and $\bar{\nu}(E) = 4$ respectively.

▸ J. Terrell

Phys. Rev. **108**, 783 (1957)

A. Tudora PbP & DSE calculations showed the same behavior of ρ_X for ^{232}Th & ^{238}U(γ, F)

▸ A. Veyssière

Nucl. Phys. **A199**, 45 (1973)

$$\sigma(\gamma,\ F) = \sum_{x=0}^{\nu_{max}} \sigma(\gamma,\ f\,xn),$$

- $\sigma(\gamma,\ F)$ total photofission cross section;
- $(\gamma,\ f\,xn)$ fission with emission of x PFN;
- ν_{max} the highest significant PFN multiplicity.

Terrell expressed the PFN multiplicity distribution ρ_X as:

$$\sum_{0}^{x} \rho_X = \frac{1}{2} + \frac{1}{2} f\Big(\frac{x - \overline{\nu} + 1/2 + b}{\sigma}\Big),$$

with

$$f(v) = \frac{1}{\sqrt{2\pi}} \int_{-v}^{v} \exp\Big(\frac{-t^2}{2}\Big)\, dt$$

- $\overline{\nu}$ average number of PFN emitted per fission;
- σ distribution width parameter;
- $b \lesssim 0.01$.

Thus, the cross section for photofission with emission of x PFN given by:

$$\sigma(\gamma,\ f\,xn) = \sigma(\gamma,\ F) \cdot \rho_X(\overline{\nu}, \sigma),$$

is a function of only three independent parameters: $\sigma(\gamma,\ F)$ and the PFN multiplicity parameters $\overline{\nu}$ and σ.

III.2. Energy dependent multiple-firing (MF) sorting method

Statistical treatment of multiple firing neutron coincidence events, originally developed for photoneutron reactions only as a follow-up for the Direct Neutron Multiplicity (DNM) sorting method which operates in *single-firing* conditions ▸ H. Utsunomiya, I. Gheorghe, et. al, NIM A 871, 135-141 (2017). Here we extended the method to include photofission reactions described by the Gaussian distribution of PFN multiplicities given by Terrell.

For each experimental point, we considered:

- the open (γ, xn) reaction channels, where the maximum x multiplicity $\mathtt{N}$ is determined by the incident photon energy. For the energy range here investigated, $\mathtt{N}$ varied from 0 to 3. Each reaction channel is characterized by:
  - $\sigma(\gamma, xn)$ cross section;
  - $E_{\gamma, xn}$ average photoneutron energy.
- the $(\gamma, f\,xn)$ reactions, where x takes values from 1 to $\nu_{max} \simeq 9$. The photofission channel is characterized by:
  - $\sigma(\gamma, f)$ total photofission cross section;
  - $\overline{\nu}$ and σ parameters of the Gaussian PFN multiplicity distribution;
  - $E_{\gamma, f}$ average energy of PFN. Note that the same value is considered for all PFN emission multiplicities, regardless of the fission chance.

Minimization constraints:

- $\sigma(\gamma, xn)$ free parameters
- $E_{\gamma, xn}$ free parameters
- $\sigma(\gamma, f)$ free parameter
- PFN $\overline{\nu}$ free parameter
- PFN $E_{\gamma, f}$ fixed to experimental ring-ratio value obtained in *single-firing* approximation
- PFN σ constrained to linearly dependent average of the present σ experimental results

GANT-PhotoFiss publication on energy dependent neutron multiplicity sorting procedure:

▸ I. Gheorghe, H. Utsunomiya, et. al, NIMA 1019, 165867 (2021)

III.3. Energy unfolding procedure

Final results for:

- (γ, n), $(\gamma, 2n)$, $(\gamma, 3n)$ photoneutron cross sections and $E_{\gamma, in}$ average energies of neutrons emitted in (γ, in) reactions
- (γ, F) photofission cross sections and promp-fission neutrons average energies $E_{\gamma, F}$ and multiplicity distribution parameters: mean number of PFNs per fission act and distribution width

III.3. Energy unfolding of excitation functions and average energies of neutron spectra for ^{238}U and ^{232}Th

Although the spectral density concentration in the maximum energy region of the spectra makes LCS γ-ray beams ideal for investigating photonuclear excitation functions, the measured cross section is in fact the convolution, or folding, between the true excitation function and the energy distribution of the incident beam.
Using the $L(E_\gamma, E_m)$ distribution, we express the measured cross section $\sigma^{fold}_{\gamma,kn}$ as:

$$\sigma^{\text{fold}}_{\gamma,\,kn}(E_m) = \xi \cdot \int_0^{E_{mi}} L(E_\gamma, E_m)\sigma_{\gamma,kn}(E_\gamma)\, dE,$$

where $\xi = (1 - e^{-\mu L})/\mu$ is a self attenuation correction factor determined by the linear attenuation coefficient μ and target thickness L.
The experimental excitation function is obtained by unfolding the measured folded cross section, following the iterative procedure described in ▸ T. Renström PRC 98, 054310 (2018).

$$\begin{pmatrix} \sigma^{\text{fold}}_{\gamma,\,kn\,1} \\ \sigma^{\text{fold}}_{\gamma,\,kn\,2} \\ \vdots \\ \sigma^{\text{fold}}_{\gamma,\,kn\,\mathtt{Nf}} \end{pmatrix} = \xi \cdot \begin{pmatrix} L_{11} & L_{12} & \dots & L_{1\mathtt{Mf}} \\ L_{21} & L_{22} & \dots & L_{2\mathtt{Mf}} \\ \vdots & \vdots & \ddots & \vdots \\ L_{\mathtt{Nf}1} & L_{\mathtt{Nf}2} & \dots & L_{\mathtt{NfMf}} \end{pmatrix} \cdot \begin{pmatrix} \sigma_{\gamma,\,kn\,1} \\ \sigma_{\gamma,\,kn\,2} \\ \vdots \\ \sigma_{\gamma,\,kn\,\mathtt{Mf}} \end{pmatrix}$$

III.3. PFNs multiplicity distributions - width parameter

Dependence with incident photon energy for the σ spread of PFNs multiplicity distributions in the photofission reactions on (a) ^{238}U and (b) ^{232}Th.

- present results (full black dots)
- present Los Alamos model predictions (full blue lines)
- recent HIγS LCS γ-ray beam data of Silano and Karwowski (full purple diamonds)
- Livermore positron in flight annihilation data (full red dots)
- linear fit to the present data is shown by the full black line.

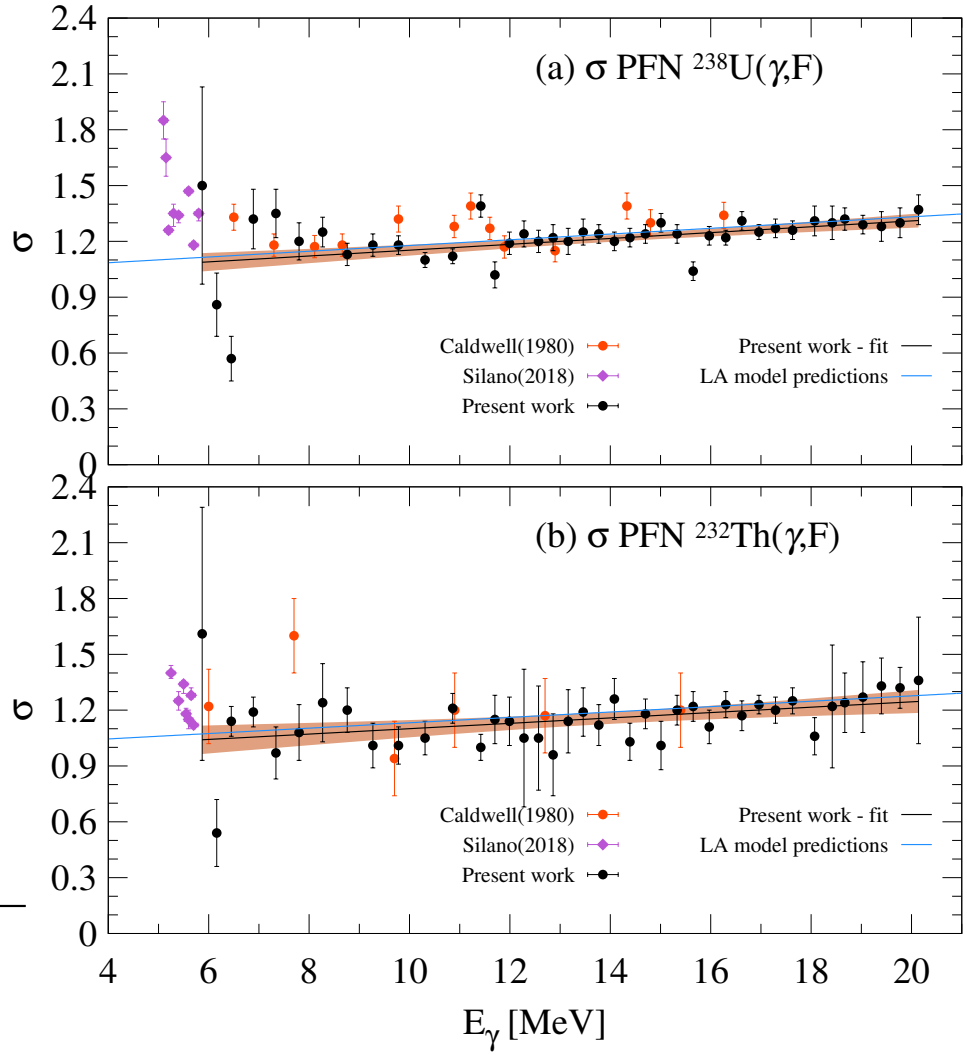

Table: Prompt fission neutrons multiplicity width parameter σ.

Target nucleus	Least squares fit to present data
^{238}U	$\sigma = 0.995 + 0.0157 \cdot E_\gamma$
^{232}Th	$\sigma = 0.956 + 0.0144 \cdot E_\gamma$

III.3. PFNs multiplicity distributions - mean parameter

- present results (full black dots)
- recent HIγS LCS γ-ray beam data of Silano and Karwowski (2018) (purple diamonds)
- Livermore data Caldwell(1980) (red dots)
- capture γ-ray data of Khan et al (1972) (brown empty squares)
- bremsstrahlung data of Findlay et al (1986) (gray open triangles)
- indirect determinations from bremsstrahlung studies of fission product yield distributions of Chattopadhyay(1973), Piessens (1993), Naik(2011,2012,2015) (blue diamonds)
- systematic linear dependences deduced from neutron-induced fission experiments by Soleilhac et al. (1969) and used by the Saclay group (Veyssiere1973) in the data reduction (green dashed-dotted lines)
- present Los Alamos model predictions (full blue lines)
- IAEA PD2019 and the ENDF/B-VIII.0 evaluations are shown in dotted black and respectively solid red lines.

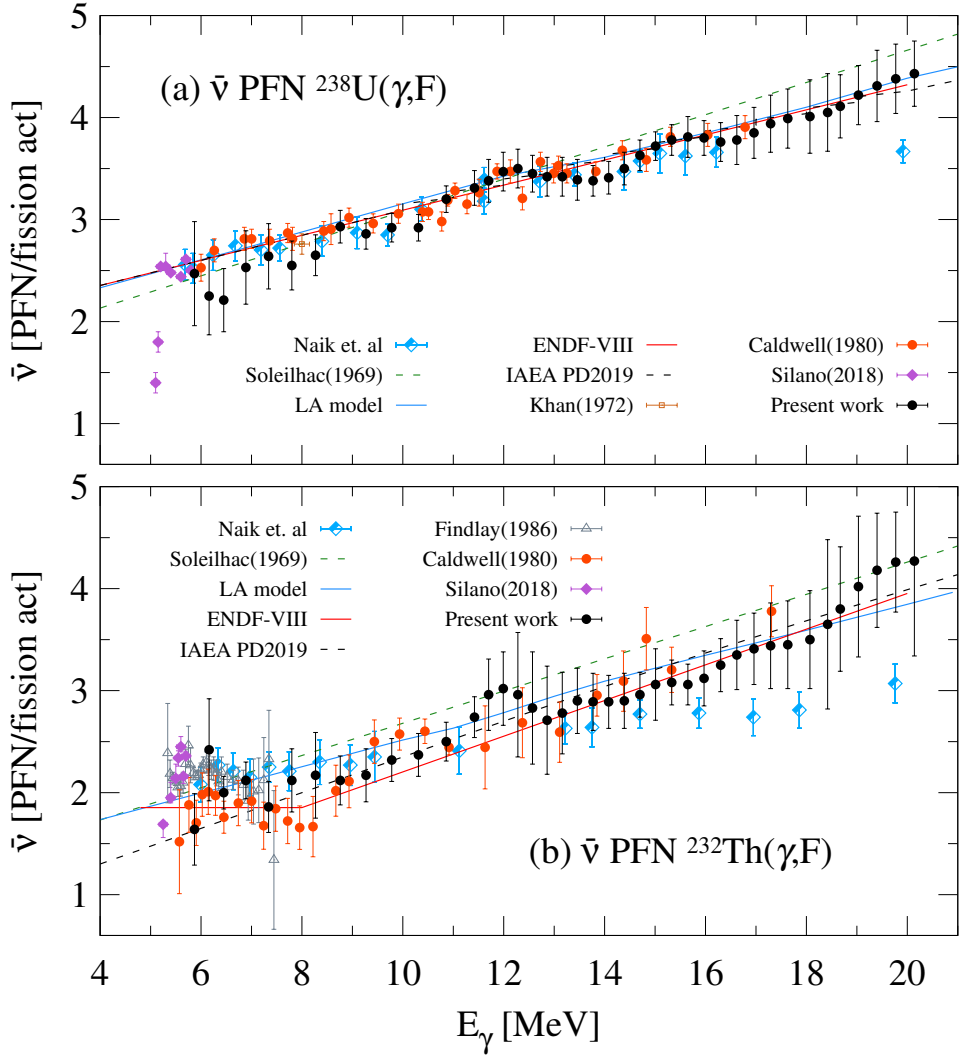

III.3. Average energies of (γ, xn) photoneutrons & PFN for ^{238}U and ^{232}Th

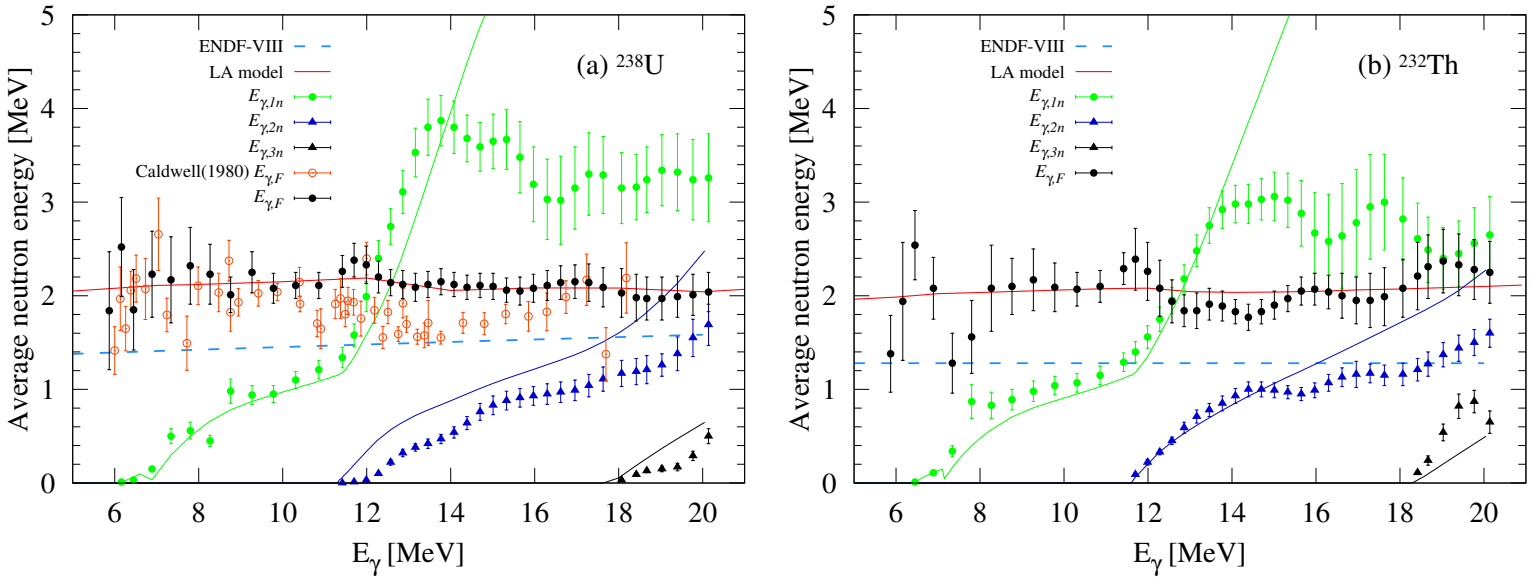

Average energies of neutrons emitted in photon induced reactions on (a) ^{238}U and (b) ^{232}Th. $E_{\gamma,\,n}$ average energy of neutrons emitted in (γ, n) reactions (green dots), $E_{\gamma,\,2n}$ for (γ, $2n$) neutrons (blue triangles) and $E_{\gamma,\,3n}$ for (γ, $3n$) neutrons (black triangles) are compared with results of present EMPIRE statistical model calculations (solid lines in corresponding color for each reaction). Present $E_{\gamma,\,F}$ PFNs energies (black dots) are compared to the ENDF/B-VIII.0 evaluation (dashed blue lines) and present Los Alamos model predictions (red lines), and, for ^{238}U, also to the results of Caldwell et al. (1980) (empty red dots).

III.3. Photoneutron and photofission excitation functions for ^{238}U and ^{232}Th

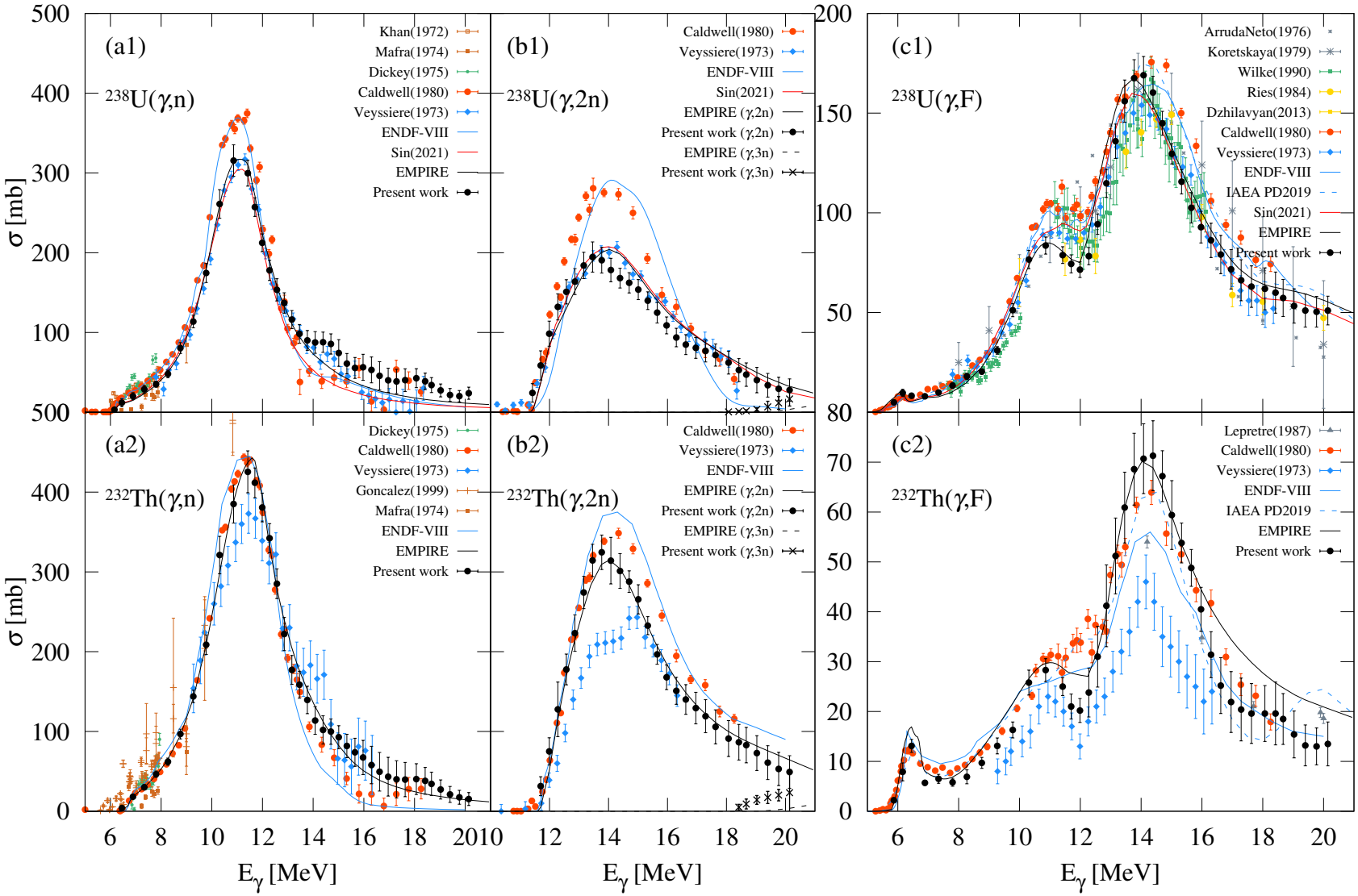

III.3. Photofission cross sections in the vicinity of S_n

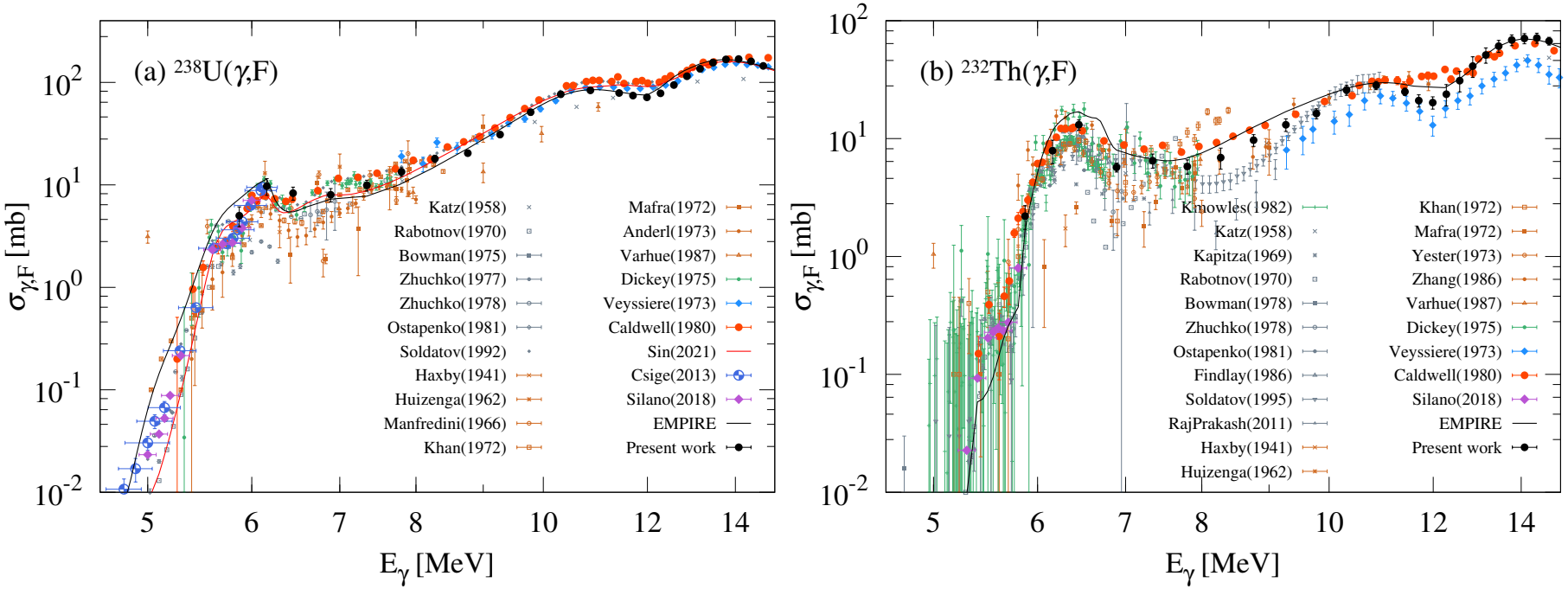

Present photofission cross sections (black full dots) for (a) ^{238}U and (b) ^{232}Th compared in the low energy region to present EMPIRE statistical model calculations (black lines) and to existing data : recent LCS γ-ray beam data obtained at HIγS by Csige et al(2013) (blue full dots) and by Silano and Karwowski (2018) (full purple diamonds) using a moderated ^{3}He detection array, the Saclay (blue full diamonds) and Livermore (red full dots) positron in flight annihilation data, bremsstrahlung data (gray symbols), bremsstrahlung monocromator data (green symbols), capture γ-ray data (brown symbols).

III.3. Photoabsorption cross sections

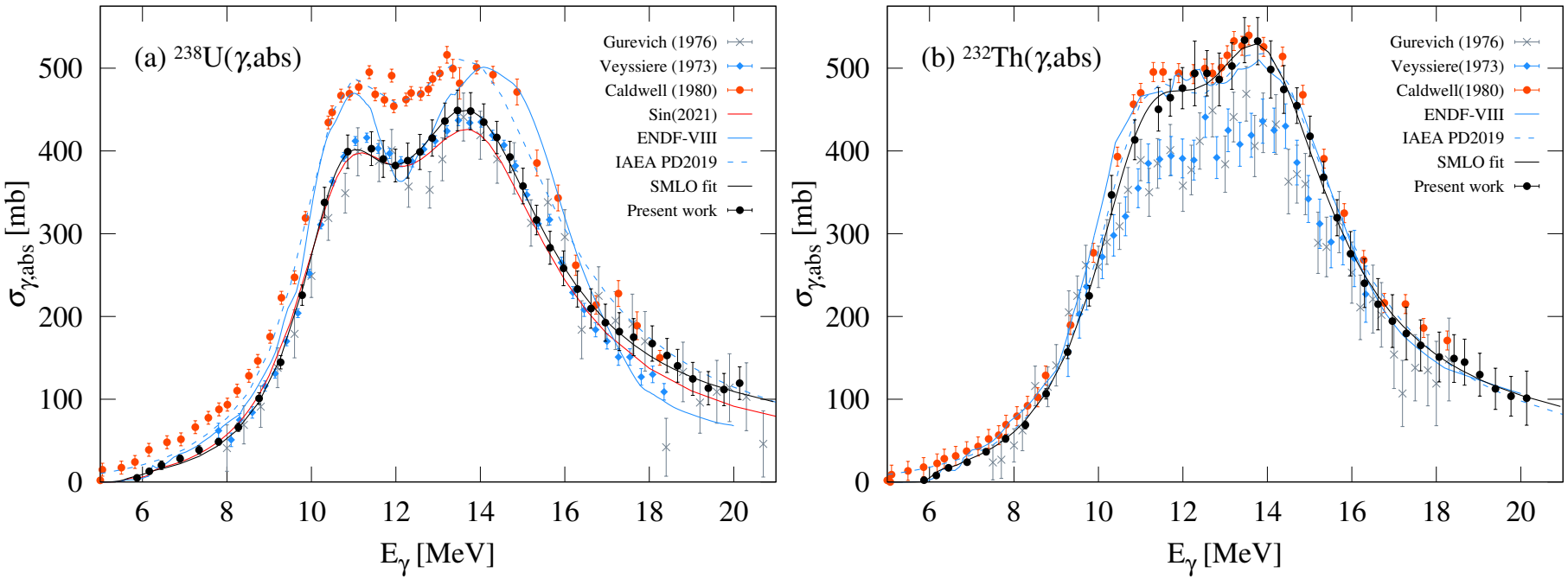

Present photoabsorption cross sections for (a) ^{238}U and (b) ^{232}Th compared to existing data obtained with positron in flight annihilation beams at Saclay (blue full diamonds) and at Livermore (red full dots) and to bremsstrahlung beam data (gray). The SMLO curves correspond to fits to the present data using the Simple Modified Lorentzian function described in by Plujko et al (2018).

Section 4

Work done during 2020 – 2023

Subsection 4

2023 – Statistical model evaluations of photon induced reactions on ^{238}U and ^{232}Th

IV.(1) Additional work: Investigate effects of fission induced by PFN emitted in photofission

The amount of neutron multiplication through neutron-induced fission reactions occurring in the target materials as photoneutrons exit the actinide samples was investigated by GEANT4.11 neutron transport simulations performed for realistic Maxwell PFNs spectra and typical PFNs mean multiplicities. It follows from the simulation that, due to the small amount of target material, such effects are negligible.

IV.(2) Additional work: first- and second-chance fission separation

- The total photofission cross sections $\sigma_{\gamma,F}$ can be expressed in terms of the $\sigma_{\gamma,f}$ first- and $\sigma_{\gamma,nf}$ second-chance fission components:

$$\sigma_{\gamma,F} = \sigma_{\gamma,f} + \sigma_{\gamma,nf}. \tag{1}$$

- In order to describe the relative contributions of the two fission chances, we will use the first-chance probability p defined as the ratio of the first-chance photofission cross section and the total photofission cross section:

$$\mathrm{p} = \sigma_{\gamma,f}/\sigma_{\gamma,F}. \tag{2}$$

- For the first fission chance, there is a linear dependence with the excitation energy for the $E_{\gamma,f}$ average energy of PFNs and for the $\overline{\nu}_{\gamma,f}$ mean number of PFNs emitted per fission act. Thus, the $E_{\gamma,f}$ and $\overline{\nu}_{\gamma,f}$ values at excitation energies above the B_{nf} second-chance fission threshold are obtained by linear extrapolation of their values below the B_{nf}.

- The average energy of the PFNs spectrum is related to the mean number of PFNs as:

$$E_{\gamma,(xn)f} = A_0 + A_1 \cdot (1 + \overline{\nu}_{\gamma,(xn)f})^{0.5}, \tag{3}$$

where $E_{\gamma,(xn)f}$ and $\overline{\nu}_{\gamma,(xn)f}$ are the average energy and mean number of PFNs emitted in the $(x+1)$-chance photofission reaction and which do not include the prefission neutron component. Thus, the A_0 and A_1 coefficients are determined from the least squares fit to the first-chance photofission $E_{\gamma,f}$ and $\overline{\nu}_{\gamma,f}$ experimental results. Then, the $E_{\gamma,nf}$ average energy of second-chance prompt photofission neutrons can expressed in terms of the $\overline{\nu}_{\gamma,nf}$ mean number of second-chance photofission neutrons:

$$E_{\gamma,nf} = f(\overline{\nu}_{\gamma,nf}). \tag{4}$$

- The E_{prefiss} energy of the prefission neutron can be estimated from the experimental $E_{\gamma,n}$ average energies of photoneutrons at low excitation energies.

IV.(2) Additional work: first- and second-chance fission separation

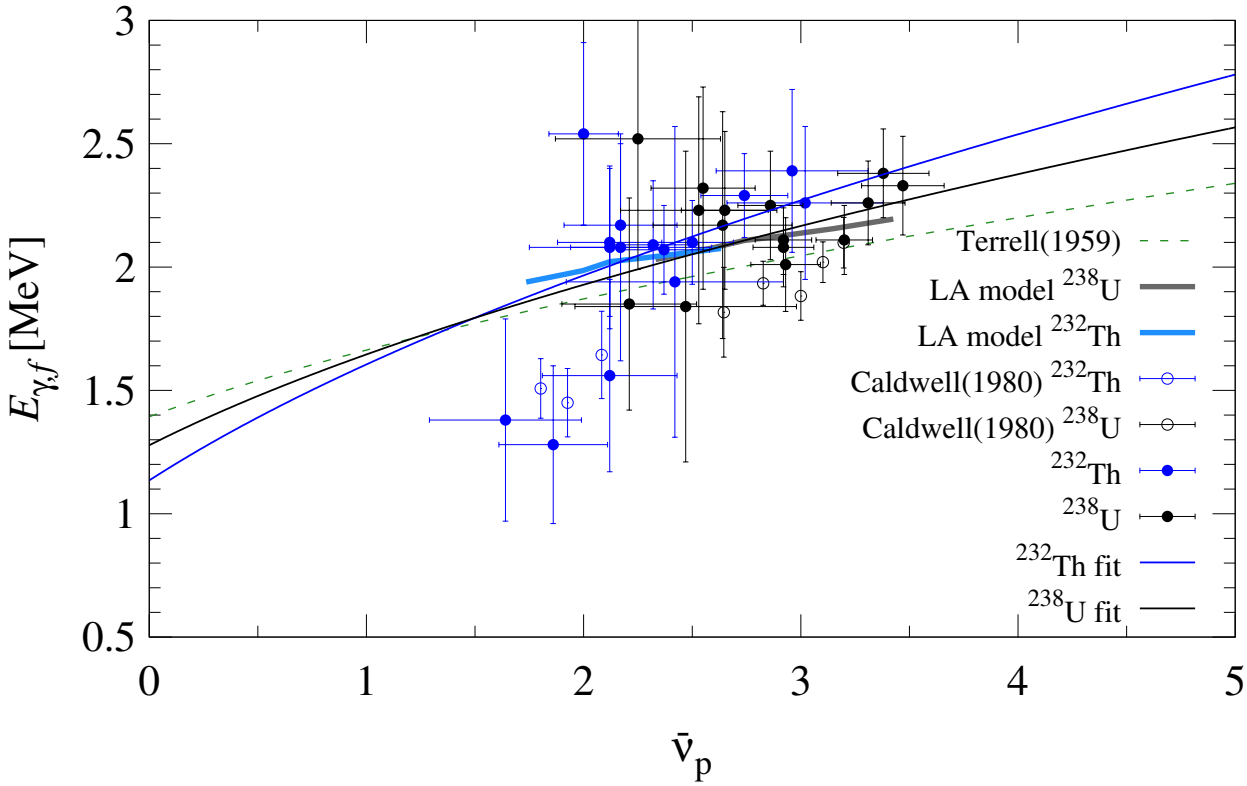

Average energy of PFNs emitted in first-chance photofission reactions on ^{238}U (black) and ^{232}Th (blue) vs the $\overline{\nu}_p$ mean number of PFNs. Present experimental results are shown by full dots and their least square fit by solid lines. Present Los Alamos model predictions are given in dotted lines and the general approximation given by J. Terrell(1959) is shown by the green dashed-dotted line.

IV.(2) Additional work: first- and second-chance fission separation

Dependence with incident photon energy for the mean PFNs multiplicities in the photofission reactions on (a) ^{238}U and (b) ^{232}Th. The present results for the $\overline{\nu}_p$ total mean number of PFNs per fission act (full black dots) and for the second chance contribution including the prefission neutron (red full dots) are compared with the corresponding Los Alamos model predictions.

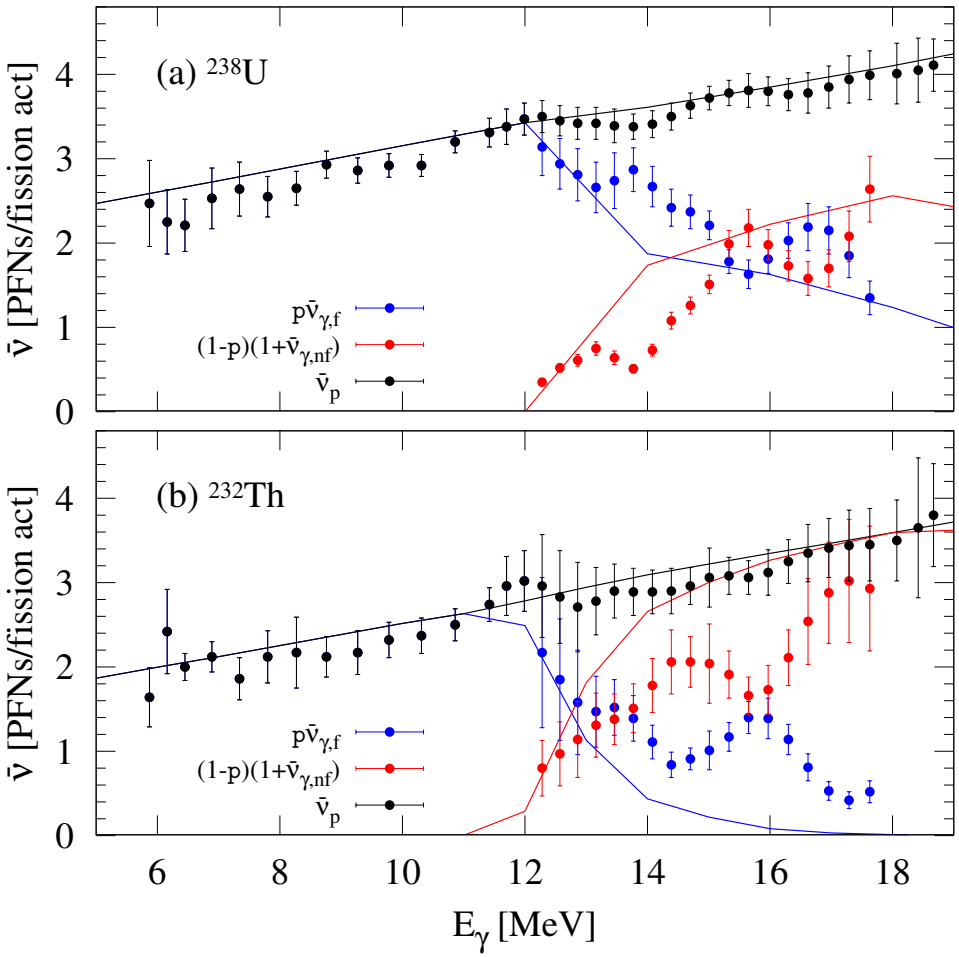

IV.(2) Additional work: first- and second-chance fission separation

Ratios of the first-chance photofission cross section to the total photofission cross section given by the sum of $\sigma_{\gamma,f}$ first- and $\sigma_{\gamma,nf}$ second-chance photofission cross sections for (a) ^{238}U and (b) ^{232}Th. Present data (full black dots) are compared with the results of Caldwell et al (1980) (red empty dots) and to present (black lines) and Sin et al. (2021) (red line) statistical model calculations.

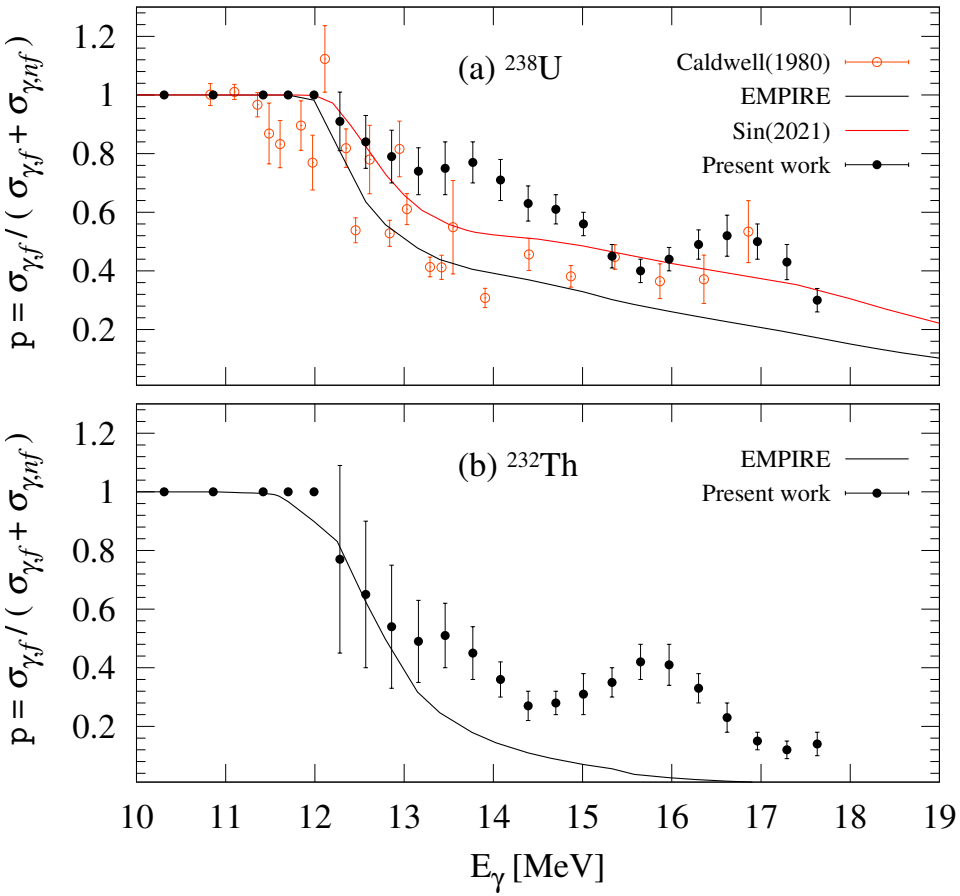

IV.(2) Additional work: first- and second-chance fission separation

Photofission cross sections for (a) ^{238}U and (b) ^{232}Th: total photofission cross sections $\sigma_{\gamma,F}$ (black), first-chance (blue) and second-chance (red) photofission cross sections. Present measurements (full dots) are compared to experimental results of Caldwell et al. (1980) (empty dots) and present EMPIRE statistical model calculations (solid lines).

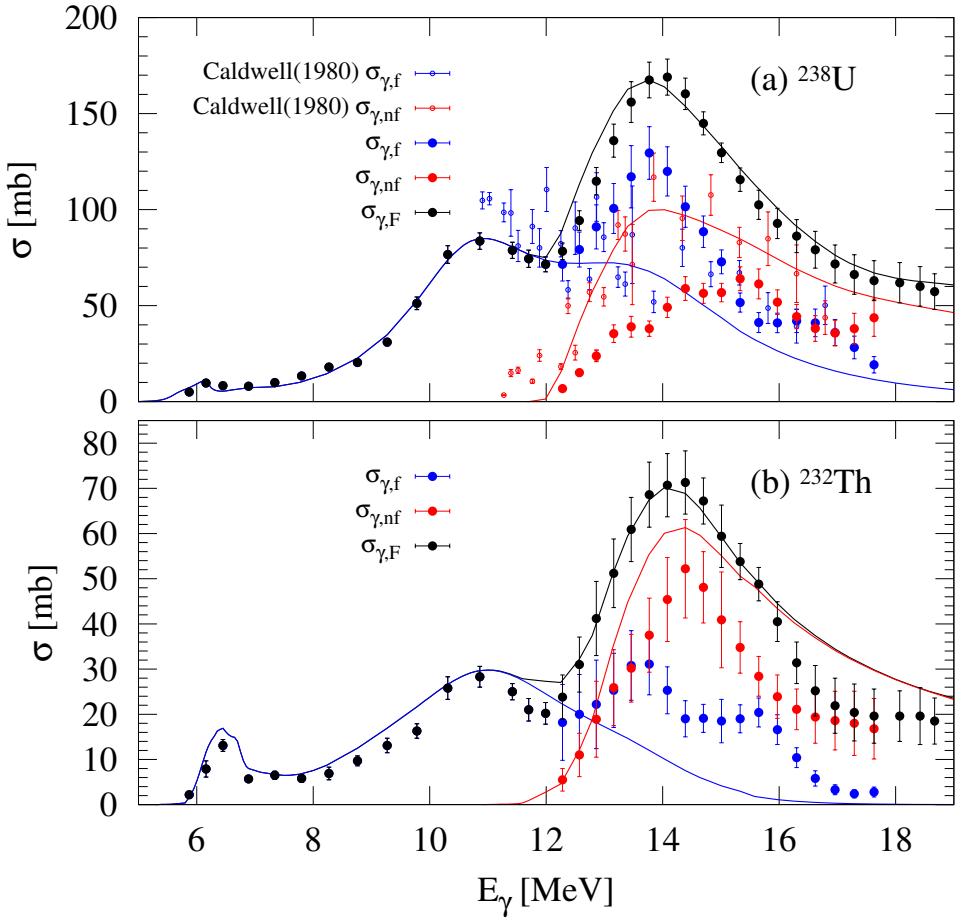

IV.(2) Additional work: first- and second-chance fission separation

Neutron to fission branching ratio Γ_n/Γ_f as a function of the excitation energy for (a) ^{238}U and (b) ^{232}Th. Present data (full black dots) are compared to the results of Caldwell et al. (1980) (red empty dots) and of Veyssiere et al. (1973) (full blue diamonds), and to statistical model calculations: present EMPIRE calculations (black lines) and the ones of Sin et al. (2021) (red line).

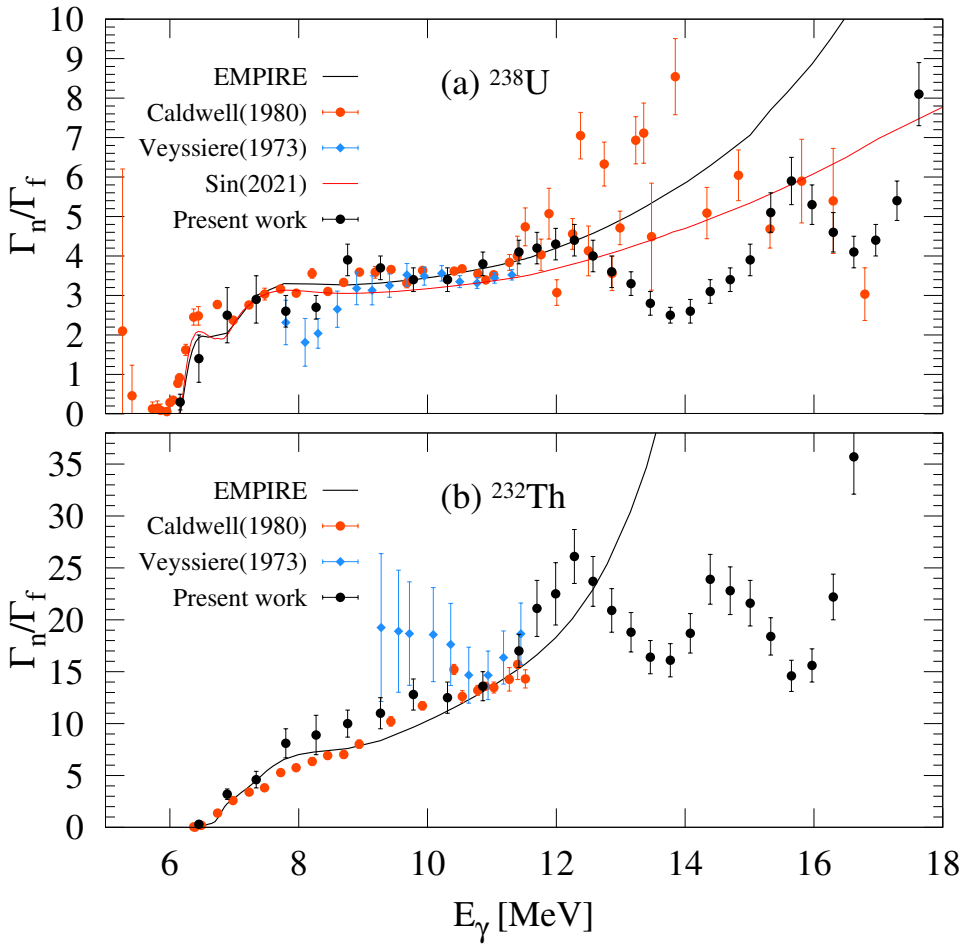

IV. Statistical model calculations

- The present photoabsorption cross sections have been fitted with several Lorentzian-type closed-forms (SLO, MLO1, SMLO) plus the quasi-deuteron contribution for the E1 γ-ray strength functions. For both ^{238}U and ^{232}Th we have found that the SMLO fit reproduces best the experimental data, especially in the low energy region. Table below gives for each nucleus the fit values of the two Lorentzian centroids, widths and peak cross sections and the normalization factor for the quasideuteron photo-absorption cross section.
- Specific optical model (OM) potentials for ^{238}U (RIPL ID - 2413) and ^{232}Th (RIPL ID - 2412) have been used to obtain the transmission coefficients for neutron emission. The level densities, both at the equilibrium deformation and at the saddle points, have been described with the enhanced generalized superfluid model (EGSM) with parameters adjusted to discrete levels.

IV. Statistical model calculations

Table: GDR parameters for ^{232}Th and ^{238}U obtained by fitting the present photoabsorption results with a SMLO function described in Plujko (2018).

CN	E(1) (MeV)	Γ(1) (MeV)	$\sigma(1)$ (mb)	E(2) (MeV)	Γ(2) (MeV)	$\sigma(2)$ (mb)	QD
^{232}Th	11.45	3.92	373.6	14.10	3.75	359.9	1.
^{238}U	10.70	2.10	246.6	13.69	5.34	399.1	3.

IV. Statistical model calculations

- The fission probabilities were computed in the frame of the Optical Model for Fission (OMF), which models the coupling between the states at fundamental deformation with the super- and hyper-deformed states as well as the vibrational states damping with the increase in the excitation energy. The fission barriers heights and widths for the first compound nuclei ^{238}U and ^{232}Th have been fixed by reproducing the existing fission cross sections in the sub-barrier region. The properties of the 1^- and 0^- discrete transition states were obtained by reproducing the sub-barrier fission resonances.
- For both nuclei, we increased the first neutron emission preequilibrium contribution computed within the PCROSS model in order to reproduce the present (γ, n) cross sections at excitation energies above ∼14 MeV. Finally we tuned the fission barrier parameters for the second compound nuclei ^{237}U and ^{231}Th in order to reproduce the interplay between $\sigma_{\gamma,\,in}$ with i = 1 – 3 and $\sigma_{\gamma,\,F}$. The fission barrier parameters used in the present EMPIRE calculations are listed in Table below. We note small differences between the present fission barrier parameters for the U isotopes and the ones obtained by Sin *et al.* (2021) by following the Saclay and bremsstrahlung data.

IV. Statistical model calculations

Table: Fission barrier parameters used in present EMPIRE calculations. $V_1(\hbar\omega_1)$, $V_2(\hbar\omega_2)$ and $V_3(\hbar\omega_3)$ are the fission barrier heights (curvatures). $V_{\rm II}(\hbar\omega_{\rm II})$ and $V_{\rm III}(\hbar\omega_{\rm III})$ are second and third well heights (curvatures) at super- and hyper-deformations [2].

Nucleus	V_1	$\hbar\omega_1$	$V_{\rm II}$	$\hbar\omega_{\rm II}$	V_2	$\hbar\omega_2$	$V_{\rm III}$	$\hbar\omega_{\rm III}$	V_3	$\hbar\omega_3$
^{238}U	6.15	1.00	1.30	1.00	5.50	0.60				
^{237}U	5.35	0.50	2.30	1.00	5.70	1.50	5.57	1.00	5.70	1.50
^{232}Th	5.80	0.70	4.75	0.30	6.00	1.70	5.20	0.90	6.00	1.70
^{231}Th	6.00	0.70	3.00	1.00	6.30	1.50				

[1] all values are given in MeV.
[2] all values are given in MeV.

Section 5

Future plans

Future plans

Giant Dipole Resonance photofission and photoneutron reactions in ^{238}U and ^{232}Th

D. Filipescu,[1,*] I. Gheorghe,[1] K. Nishio,[2] T. Ohtsuki,[3] H. Wang,[4] G. Fan,[4] S. Goriely,[5] A. Tudora,[6] K. Stopani,[7] H. Suzaki,[2] K. Hirose,[2] M. Inagaki,[3] M. Bjørøen,[8] Y.-W. Lui,[9] T. Ari-izumi,[10] S. Miyamoto,[11] and H. Utsunomiya[10,†]

[1] *National Institute for Physics and Nuclear Engineering, Horia Hulubei (IFIN-HH), 30 Reactorului, 077125 Bucharest-Magurele, Romania*
[2] *Advanced Science Research Center, Japan Atomic Energy Agency, Tokai, Ibaraki 319-1195 Japan*
[3] *Institute for Integrated Radiation and Nuclear Science, Kyoto University, 2-1010 Asashiro-nishi, Kumatori, Sennan, Osaka 590-0494, Japan*
[4] *Shanghai Advanced Research Institute, Chinese Academy of Sciences, No.99 Haike Road, Zhangjiang Hi-Tech Park, 201210 Pudong Shanghai, China*
[5] *Institut d'Astronomie et d'Astrophysique, Université Libre de Bruxelles, Campus de la Plaine CP 226, 1050 Brussels, Belgium*
[6] *University of Bucharest, Faculty of Physics, str. Atomistilor 405, Bucharest-Magurele, Jud. Ilfov, 077125, Romania*
[7] *Lomonosov Moscow State University, Skobeltsyn Institute of Nuclear Physics, 119991 Moscow, Russia*
[8] *Department of Physics, University of Oslo, N-0316 Oslo, Norway*
[9] *Cyclotron Institute, Texas A&M University, College Station, Texas 77843, USA*
[10] *Konan University, Department of Physics, 8-9-1 Okamoto, Higashinada, Kobe 658-8501, Japan*
[11] *Laboratory of Advanced Science and Technology for Industry, University of Hyogo, 3-1-2 Kouto, Kamigori, Ako-gun, Hyogo 678-1205, Japan*

(Dated: November 1, 2023)

New measurements of photofission and photoneutron reactions on ^{238}U and ^{232}Th in the Giant Dipole Resonance (GDR) energy region have been performed at the laser Compton-scattering γ-ray source of the NewSUBARU synchrotron radiation facility using a high-and-flat efficiency moderated ^{3}He detection array. The neutron-multiplicity sorting of high-multiplicity fission neutron coincidence events has been performed using a dedicated energy dependent, multiple firing statistical treatment. The photoneutron (γ, in) with $i = 1 - 3$ and photofission (γ, F) reactions have been discriminated by considering a Gaussian distribution of prompt-fission-neutron (PFN) multiplicities predicted by the theory of evaporation in sequential neutron emission from excited fission fragments. We report experimental (γ, n), $(\gamma, 2n)$, $(\gamma, 3n)$ and (γ, F) cross sections, average energies of PFN and of (γ, in) photoneutrons, as well as the mean number of PFN per fission act and the width of the PFN multiplicity distribution. Based on these primary experimental results and combined with reasonable assumptions, we extract also the first- and second-chance fission contributions. The new experimental results are compared with statistical-model calculations performed with the EMPIRE-3.2 Malta code on the present data and with prompt fission emission calculations obtained with the Los Alamos model in the frame of the most probable fragmentation approach with and without sequential emission.

Submit the ^{238}U and ^{232}Th paper to PRC by the end of 2023.

Section 6

Summary

Summary

Achieved all objectives:

- Theoretical modeling of PFN multiplicities and energy spectra – ▸ ND2022 contribution of A.Tudora – UB partner;
- Developed neutron multiplicity sorting procedure for photofission and photoneutron measurements with flat efficiency moderated neutron detection arrays of the ELIGANT-TN type – ▸ I. Gheorghe et al., Updated neutron-multiplicity sorting method, NIM A **1019**, 165867 (2021).
- Developed associated LCS γ-ray beam diagnostics procedure:
  - ▸ D. Filipescu et al., Spectral distribution and flux of LCS γ-ray beams, NIM A **1047**, 167885 (2023), arXiv:2211.14650
  - ▸ D. Filipescu, Monte Carlo simulation of LCS polarization effects, JINST **17** P11006 (2022), arXiv:2210.14669
  - ▸ Takashi Ari-Izumi et al., Spatial distribution of collimated LCS γ-ray beams, JINST **18** T06005 (2023), arXiv:2304.08935
- Applied the procedures on experimental ^{238}U and ^{232}Th data taken at the NewSUBARU LCS γ-ray beam line. Produced experimental photoneutron and photofission cross sections $\sigma_{\gamma,xn}$ and $\sigma_{\gamma,fxn}$ as well as average neutron emission energies $E_{\gamma,xn}$ and E_{PFN}, PFNs multiplicity distribution parameters (mean and width) as well as first- and second-chance fission separation – ▸ ND2022 contribution of D. Filipescu and PRC paper to be submitted.
- Performed EMPIRE statistical model calculations on photoneutron and photofission reactions on ^{238}U and ^{232}Th.

Equipment acquired within the project:

- electronic module – multichannel shaper, TFA, CFD
- accessories (cabling)

for neutron multiplicity sorting experiments at IFIN-HH with ELIGANT-TN type of detection systems.

Thank you for your attention!